19th World Congress of Soil Science

Symposium 1.6.1
Impact of aelian sediments on pedogenesis

Soil Solutions for a Changing World,

Brisbane, Australia

1 – 6 August 2010

Table of Contents

Aeolian salinization of soils on the piedmont plain of Eastern Tian Shan (Lake Ebinur area, China)

Mariya V. Konyushkova[A], Jilili Abuduwaili[B] and Ivan P. Aidarov[C]

[A]V.V. Dokuchaev Soil Science Institute RAAS, 7 Pyzhevskii per., Moscow, 119017 Russia, Email mkon@inbox.ru
[B]Xinjiang Institute of Ecology and Geography CAS, 40-3 South Beijing Road, Urumqi, 830011 China, Email jilil@ms.xjb.ac.cn
[C]Moscow State University of Environmental Engineering, 19 Pryanishnikova St, Moscow, 127550 Russia, Email ivan@aidarov.com

Abstract
This study is focused on the effect of aeolian transport on soil formation and salinization in the piedmont plain of the northern slope of Tian Shan (Xinjiang-Uygur Autonomous Region of China). On the basis of the data on aeolian input of dust and salts (determined by dust collectors) and soil salinity at the 300-km transect it is shown that soil formation and salinization is closely related to aeolian processes. The main source of aeolian material is the dried up bottom of Lake Ebinur (wet playa). Maximum soil salinity (3-6% of salts) is observed in the soils near Jinghe settlement where the maximum aeolian input of salts is also registered. In the soils beyond 100 km from the dried bottom of the lake, salt content is low (0.1-0.4%). Chemical composition of salts in the soils is related to chemical composition of aeolian material. Chloride salts prevail in the soils located in the areas with the high Cl^- to SO_4^{2-} ratios (from 0.8 to 1.5) in aeolian salts. In places with a predominance of sulphates in the composition of aeolian salts, soils are characterized by the sulphate type of salinization. Preliminary calculations show that the formation of the modern profile of the studied soils takes about 2000 years.

Key Words
Central Asia, Dzungarian Gate, aeolian genesis of soils, desert soils, Holocene history

Introduction
The genesis of salts in the soils formed on the gravelly deposits of piedmont plains in Central Asia is an argued issue. The influence of two main factors determining the salinity of overwhelming part of salt-affected soils of the world - salinity of parent rocks and ground water - is absent here. The existing hypothesis of aeolian genesis of salts in those soils (Nosin, 1960; Pankova, 1992) has not been supported by experiments.

In this study we have tried to estimate the effect of the aeolian factor on soil salinity in the piedmont plain of the northern slope of Eastern Tian Shan (Xinjiang Uygur Autonomous Region of China) on the basis of the data on the content and composition of salts in aeolian material and soils. This study is the continuation of the series of research devoted to the reasons and influence of Lake Ebinur desiccation on surrounding landscapes.

Materials and methods
The piedmont plains of the northern slope of Tian Shan occupy altitudes from 250 to 700 m a.s.l. They are represented by alluvial and colluvial fans and are mainly composed of coarse gravelly material. In the lower part of piedmont plains (250-350 m a.s.l.), the deposits are often represented by loess of different thickness. Natural vegetation of piedmont plains is sparse, consists of saxaul (*Haloxylon persicum, Haloxylon ammodendron*), tamarix (*Tamarix ramosissima*), saltworts (*Kalidium foliatum, Kalidium cuspidatum, Kalidium caspicum*), wormwood (*Artemisia* sp.). The depth of ground water is 15-30 m and more.

Climate is arid with mean annual precipitation 100-200 mm and potential evaporation 1500-2000 mm. Maximum precipitation falls in summer. Snow cover is shallow, 10-25 cm. Mean July temperature is +27°C, mean January temperature is -17°C. Strong winds are frequent. The amount of days with the winds >8m/s is 164 per year (Guijin Mu et al., 2002). The winds predominantly have northwestern direction; they come to the Dzungarian (or Junggar) Basin in the area of northwestern part of Lake Ebinur from Dzungarian Gate - a relatively narrow pass between the ridges of the Dzungarian Alatau and the Western Dzungarian Mountains (Figure 1).

1 – 6 August 2010, Brisbane, Australia. Published on DVD.

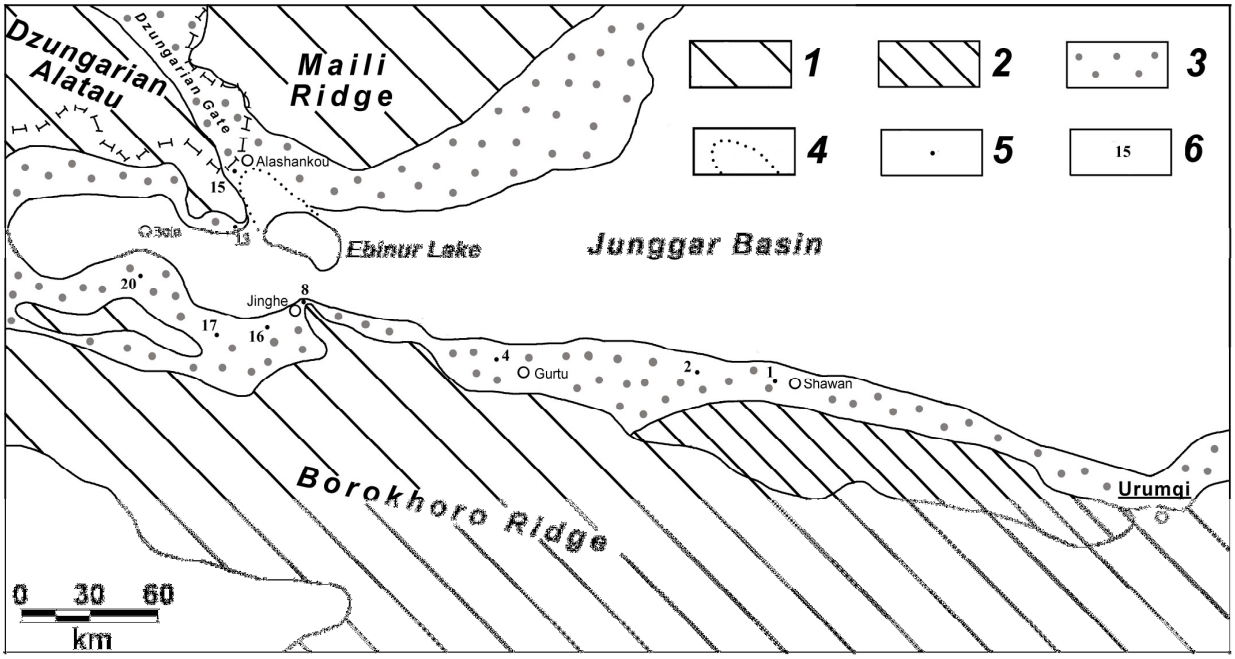

Figure 1. Study area. Legend: 1 - mountains, 2 - outcrops of loose saline Tertiary deposits, 3 - piedmont plain, 4 - dry lakebed, 5 - pits location, 6 - numbers of pits.

Lake Ebinur is located in the northwest of China, in the west of Dzungarian Basin, at the altitudes about 190 m a.s.l. The lake is a closed salt lake with chloride-sulphate composition of water, 80-120 g/l (Fan Zili and Zhang Leide, 1992). The average depth of the lake is 2-3 m, maximum 5 m. In the middle Holocene (some 5000 ago), at the place of the modern salt lake, a fresh lake with the area of 3000 km^2 and depth of 40 m existed. In the late Holocene, the area of the lake began to decrease due to the decreased surface runoff; by the beginning of the XX century, its area was 1300 km^2. Since the 1950s, anthropogenic activity (increase in consumption of surface water for irrigation and domestic use) added to the desiccation of the lake. At the beginning of the XXI century, the area of the lake is about 600 km^2. The surface released from water represents a vast bare wet playa with very high salinity (>40% of salts in the upper 2 cm, 10-30% in the layer of 2-5 cm). The composition of salts is chloride-sulphate with sodium (Abuduwaili Jilili and Guijin Mu, 2006). The northwestern wind blowing from Dzungarian Gate entrains salty dust and transports it to tens and hundreds of kilometres from the lake.

The previous studies have shown that the main source of aeolian material on the piedmont plains is the dried bottom of Lake Ebinur (Guijin Mu et al., 2002; Abuduwaili Jilili and Guijin Mu, 2006; Abuduwaili Jilili et al., 2008). The aeolian transport was studied in 1998-1999 at a 300-km-long transect. At 13 sites including Alashankou, Bortala (Bole), Jinghe, Gurtu, Shawan and several settlements between them, dust collectors were established. Samples were collected each month. It was revealed that the amount of aeolian dust fall is dependent on the position of a sampling site relative to the lake, distance from the lake and the location of the obstacles relative to wind flow. Maximum dust fall (400-600 t/km^2/a) is registered in the zone of wind retardation due to a barrier in the form of a bulging ridge of the Tian Shan at the Jinghe sampling site. At the other sites (the farthest one, Shawan, is located 230 km from the lake), aeolian dust fall is 100-200 t/km^2/a.

The total amount of salts in the aeolian material is high and reaches 10–25%. Salts are mostly represented by calcium and sodium chlorides and sulfates. The maximum amount of salts (77 g/m^2/a) is deposited at Jinghe; at the other sites, the deposition of salts varies from 14 to 27 g/m^2/a. The analysis of the chemical composition of salts reveals certain regularity in aeolian transport of salts. At long distances from the source of the eolian material, calcium sulfate predominates in the composition of salts; at closer distances, sodium chloride is actively deposited together with calcium and sodium sulfates.

At different distances and directions from Lake Ebinur, 9 soil pits were studied. According to the Russian and Chinese soil classifications, the soils belong to gray-brown desert type. According to WRB, they are correlated to Calcisols and Gypsisols. For soil samples, the content of Cl^-, SO_4^{2-}, HCO_3^-, Ca^{2+}, Mg^{2+}, Na^+, K^+ in water extract (1:5), pH, particle-size distribution, humus, gypsum, and carbonate contents were examined.

Results

Soil salinity

The studied soils have the following morphology:
0-3 cm - porous crust, dry, light pale yellow, with gravel, effervescent;
3-10 cm - very fine platy, dry, pale brown, with gravel;
10-25 cm - crumby, pale brown, with gravel;
>25 cm - gravel with gypsiferous "beards" on the lower side of stones, fine earth between the stones.

The depth of fine earth (silt loam) horizons can decrease to 10-12 cm. In pit 15 located in Dzungarian Gate, where predominant removal of loose material takes place, fine earth horizon is absent; fine material is entrapped only between stones. The humus content in soils is low - from 0.3 to 0.9%, 0.4% on average. Soils have high pH - from 9 to 10, rarely from 8 to 9. A horizon of maximum salt accumulation is observed from 3-8 cm and has the total thickness of 5-10 cm (Figure 2). Surface crust (maximum 3 cm) is free from salts.

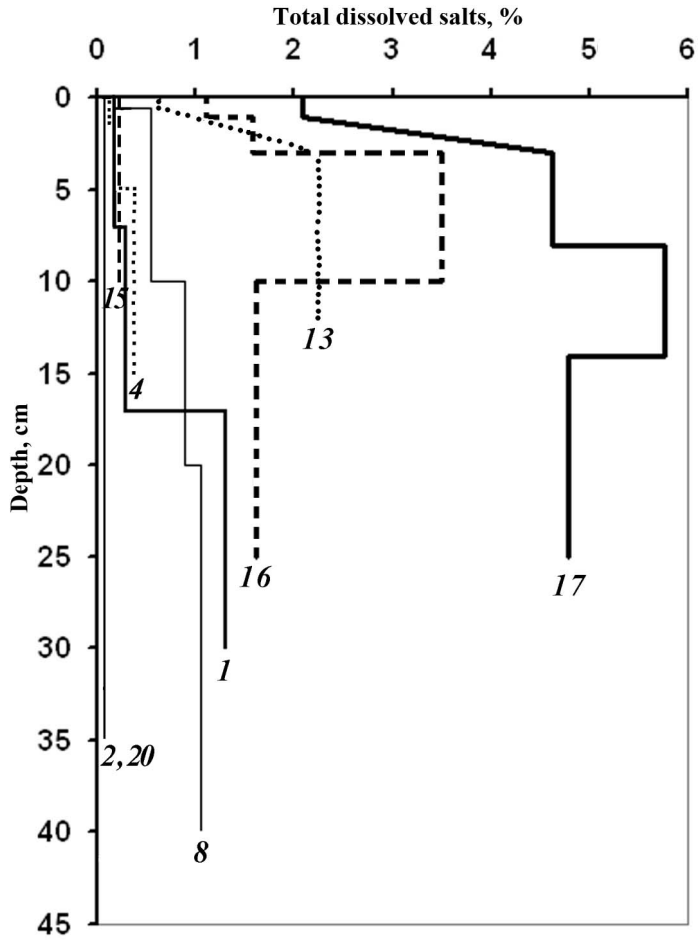

Figure 2. Dissolved salts content in gray-brown desert soils of the piedmont plain of Eastern Tian Shan. Numbers indicate a number of a pit. Pit 1 is underlain from 17 cm by dislocated saline deposits.

The salt content of the studied soils is various and closely related to the input of aeolian salts. Thus, the maximum salinity (3.5-5.8% of salts) is found in Pit 16 and 17 located near Jinghe. As shown above, the maximum aeolian salt input is prominent in this area. Less but still high soil salinity is observed in Pit 13, where aeolian salt input is quite high (about 30 t/km^2/a). In Pit 8, which is located close to Jinghe, soil salinity is lower than in the adjacent pits - <1%. This pit, in contrast to other studied soils, is located in the shallow valley of the terminal (seasonal) stream. Thus, spring water removed salts from soil profile. In other soils, the salt content is low - from 0.1 to 0.4%.

Chemical composition of salts in the soils is related to chemical composition of aeolian material. Thus, chloride salts prevail in the soils located at the areas where high Cl^- to SO_4^{2-} ratios (from 0.8 to 1.5) in aeolian salts are registered. At the places where sulphates predominate in aeolian salts, soils have a sulphate composition of salts.

Model of aeolian soil formation and salt accumulation
We have tried to estimate approximately the time of the existing soils formation on gravelly deposits due to aeolian input of dust. It was calculated according to the formula of Golovanov et al. (2001), which accounts for transport of particles in soils under the action of water (Formula):

$$t = \frac{\omega(1+\alpha)}{\alpha V(8\lambda + L)}\left[1 - \sqrt{\frac{L^2}{(8\lambda + L)^2}}\right]$$

where t is the time of penetration of aeolian dust into coarse deposits to the depth of 30 cm, days; α is a factor of fine particles (<0.02 mm) adhesion with the coarse material (equal to 0.01); λ is a factor of hydrodynamic dispersion (characterizes the transport with water in porous media, depends on texture) (equal to 0.001); V – real infiltration rate (equal to 0.000003 m/day); ω – volume water content in the layer of periodical moistening (equal to 0.008); L – the depth of penetration of fine particles (<0.02 mm) (equal to 0.3 m).

After inserting the values into the formula, we get that the formation of existing soils takes about 1850 years. Close figures (about 2000 years) are obtained when calculating the time of salt accumulation from zero to the present values. We realize that the calculated figures are very approximate, but they are quite concordant with paleogeographic data on the lake dynamics in Holocene.

Conclusions
1. Salinity of gray-brown desert soils on the gravelly deposits of the piedmont plain in the northern slope of Tian Shan varies from slight to very strong levels.
2. Soil salinity is related to aeolian input of salts from the dried bottom of Lake Ebinur. The degree of salinization reaches its maximum in the soils where intensive aeolian salt deposition is registered. At the distance beyond 100 km from the dry lakebed, soils are slightly saline.
3. Chemical composition of salts in soils is various - sulphate, chloride-sulphate, sulphate-chloride and chloride. It is related to chemical composition of aeolian material too.
4. According to our calculations, the formation of studied gray-brown desert soils on gravelly deposits took 2000 years. This date is in good correlation with paleogeography of the study area.

Acknowledgment
This study was supported by the Russian Foundation for Basic Research (grant No. 07-04-00136).

References
Abuduwaili Jilili, Gabchenko MV, Junrong Xu (2008) Eolian transport of salts - a case study in the area of Lake Ebinur (Xinjiang, Northwest China). *Journal of Arid Environments* **72** (10), 1843-1852.

Abuduwaili Jilili, Guijin Mu (2006) Eolian factor in the process of modern salt accumulation in Western Dzungaria, China. *Eurasian Soil Science* **39** (4), 367-376.

Fan Zili, Zhang Leide (1992) A study on the hydrochemistry of lakes in Xinjiang. *Arid Zone Research* **9** (3), 1-9. [in Chinese, with English abstract].

Golovanov AI, Surikova TI, Sukharev YuI (2001) Fundamentals of Environmental Engineering. 283 p. (Kolos: Moscow) [in Russian].

Guijin Mu, Shun Yan, Abuduwaili Jilil, Qing He & Xuncheng Xia (2002) Wind erosion at the dry-up bottom of Aiby Lake – A case study on the source of air dust. *Science in China (Series D)* **45** (Supp. P), 157-164. [in Chinese].

Nosin VA (1960) On the zonal type of soils in the southwestern part of Dzungarian Basin. In 'Natural Conditions in Xinjiang', pp. 41-65. (Izd. Akad. Nauk SSSR: Moscow) [in Russian].

Pankova YeI (1992) Genesis of soil salinization in deserts. 136 p. (Moscow) [in Russian].

Chronosequence of postglacial soil paleocatenas in the dune area of the Toruń Basin (Northern Poland)

Michał Jankowski

Faculty of Biology and Earth Sciences, Nicolaus Copernicus University, Toruń, Poland, Email mijank@umk.pl

Abstract
The paper presents structure and interpretation of combined chronosequence of soil paleocatenas, formed in the postglacial period in the inland dune area of the Toruń Basin (Northern Poland, Central Europe). Based on radiocarbon, palynological and archaeological datings, four generations of paleosols were distinguished, of Alleröd, Preboreal, Eo-Mesoholocene and Neoholocene ages. Time spans of pedogenesis divide periods of aeolian activity: Late Glacial climatogenic period with three phases: pre-Alleröd, Younger Dryas and late Preboreal and anthropogenic period with episodes correlated with archaeological cultures and second-level climate oscillations, during Neoholocene. Paleosols of particular generations form similar catena patterns on dune slopes, composed of Podzols, Gleyic Podzols, Humic Gleysols and Histosols, providing diversity of geoecosystems depending on landscape position. Additionally, during Holocene two different sandy analogues of Cambisols developed: so called Finow soils (Schlaak 1993), as the effect of climate cooling at the break of Younger Dryas and Preboreal and Brunic Arenosols, as the effect of leave forest succession during Eo-mezoholocene and Neoholocene. Despite typological similarity, soils of different ages distinctly differ in stage of development, which relates to both time and conditions of pedogenesis.

Key Words
Paleocatena, Chronosequence, Paleosols, Aeolian sands, Late Glacial, Holocene

Introduction

The general scheme of stratigraphy of postglacial paleosols and aeolian sands in dune areas of Central Europe are now well recognized and described in literature (Manikowska 1991, Schirmer 1999). As an effect of aeolian sand mobility, paleosols in dunes can be preserved very easily. However, mostly only fragments of buried soil mantle, represented by single soil types are found. Studies of buried toposequences of different soils, changing depending on topographical position, can support more complex paleogeographical interpretations. Natural paleocatenas (Valentine, Dalrymple 1975) met in the field are rare objects in aeolian sands (Wilson 1987, Kaiser et al. 2006). In some cases combined toposequences can be structured using the same age paleosols from different places of well recognized landscape position.
This paper presents a combined chronosequence of soil paleocatenas developed in the dune area during Late Glacial and Holocene and its paleogeographical interpretation.

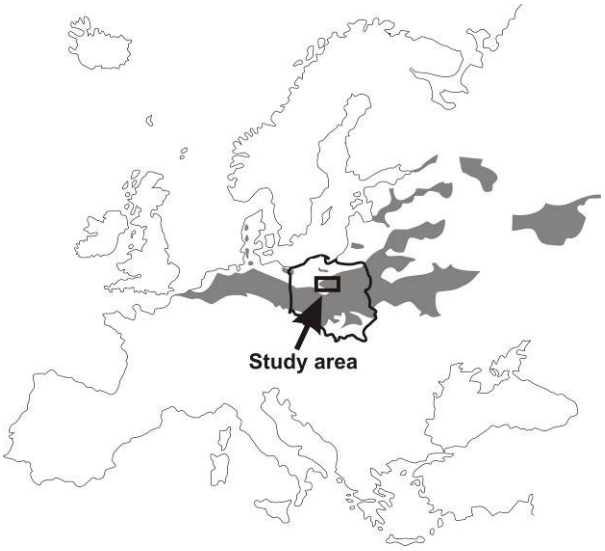

Figure 1. Location of the study area, in the European sand belt (Zeeberg 1998)

Study area, the Toruń Basin is situated in the Northern Poland, Central Europe (Figure 1). From geomorphological point of view it consists of a system of sandy, strongly windblown glaciofluvial terraces of the Toruń-Eberswalde ice-marginal stream, formed during the deglaciation after the Pomeranian phase of the last glaciation (Vistulian; ca 16 ka BP). One of the biggest inland dune fields of Europe formed there in the Late Glacial period, mostly under impact of W winds.

Methods

Numerous buried soils were documented in dunes and aeolian covers of the Toruń Basin. Three main study sites (Katarzynka, Lasek Bielański, Rudak), representing vertical sequences of different-age buried soils and five additional sites with single paleosols were chosen for further studies. Two sites (Katarzynka and Lasek Bielański) contain natural paleocatenas. The remaining study objects complement individual paleocatenas and the whole view of their combined chronosequence.

Paleosols were dated using ^{14}C radiocarbon method (13 samples of charcoals or humic material, in the Gliwice Radiocarbon Laboratory, Poland), palynological analyses (3 shallow profiles, performed by dr B. Noryśkiewicz, Institute of Geography NCU, Toruń) and on the basis of archaeological findings (2 sites, known from documentation and field studies). Soil morphology, main properties (texture, organic carbon and nitrogen contents, pH, oxalate extractable Fe_o and Al_o, total Fe_t and dithionite extractable Fe_d contents) and soil typology were determined according to standard procedures. Pedogenic characteristics of particular paleosols were reported in previous work (Jankowski 2002).

Results

In the light of radiocarbon datings, palynological and archaeological findings, paleosols of the Toruń Basin can be grouped in four generations: of Alleröd (buried ca 11100 BP), Preboreal (buried ca 9500 BP), Eo-Mesoholocene (existing on land surface during late Preboreal-Subboreal time span) and Neoholocene (developing during Subbboreal and/or Subatlantic) ages (Figure 2). Such pedostratigraphy documents also four phases of intensive aeolian activity, lasting: before Alleröd, during Younger Dryas, in late Preboreal and through the whole Subboreal and Subatlantic periods. According to results from other parts of Central Europe (Schirmer 1999) three first dune-forming phases, dividing short periods of pedogenesis, were connected to periglacial conditions during Late Glacial and the beginning of Holocene. During Neoholocene, few cycles of older soils covered with dune sands, as well as new soil formation occurred. Numerous archaeological data and also findings of cereals grains and other synanthropic plants in pollen diagrams, show anthropogenic origin of aeolian activity during last 4800 years. Sand blowing started together with the appearance of the first neolithic people who learned how to cultivate sandy soils. Records of aeolian processes, simultaneous in distant places, refer to intensification of human activity during Neolith (Funnel Beaker Culture - 4800-4500 BP), Bronze Age (Iwno Culture, 3800-3400 BP, Lusatian Culture, 3000-2900 BP) and Iron Age (Lusatian Culture, 2200-1900 BP, Middle Ages, 1300-1000 BP).

It is worth noticing, that periods of intensive human activity, as the main factor of aeolian process initiation, imposed on drier second-level climate phases during Neoholocene, could promote wind activity. Probably only during dry periods Gleysols, the most fertile among poor sandy soils, were not too wet for primitive agricultural use. On the other hand, cultivation induced wind blowing and thus burial of deforested soils.

All four generations of paleosols built similar catena patterns on buried land surfaces, for the first time formed during Alleröd on dunes and on slopes of glaciofluvial terraces. In that pattern, automorphic Podzols occupy the highest position, changing downslope into Gleyic Podzols and further into Humic Gleysols. In the most wet places Histosols developed. Such diversity of soil cover seems to prove the diversity of the whole landscape already at the beginning of post-glacial forest succession. Thus Alleröd forests, traditionally called “pine-birch” should be called rather “pine and birch”, with most pine participation in dry positions (Podzols, Gleyic Podzols) and birch in wetlands (Humic Gleysols and shallow Histosols). Alleröd shallow Histosols, often formed on surface of dead-ice blocks, after ice melting sank and now lie in inverse position – under lake sediments (gytiia; Figure 2).

In Preboreal paleocatena additionally so called “Finow soils” (Schlaak 1993), similar to Cambisols of cold climates occur in places with an autogenic regime. This probably marks environmental conditions change at the break of last cooling of the Late Glacial (Youngest Dryas) and Holocene.

In two younger generations of the Holocene age (Eo-mezoholocene and Neoholocene) the Podzol-Gleyic Podzol-Humic Gleysol-Histosol catena pattern was limited to slopes of poor dunes only. In relatively more fertile places (glaciofluvial terraces, shallow aeolian covers on erosional moraine surfaces), sandy analogues of Cambisols (Brunic Arenosols) developed, which is interpreted as an influence of leaf forests succession.

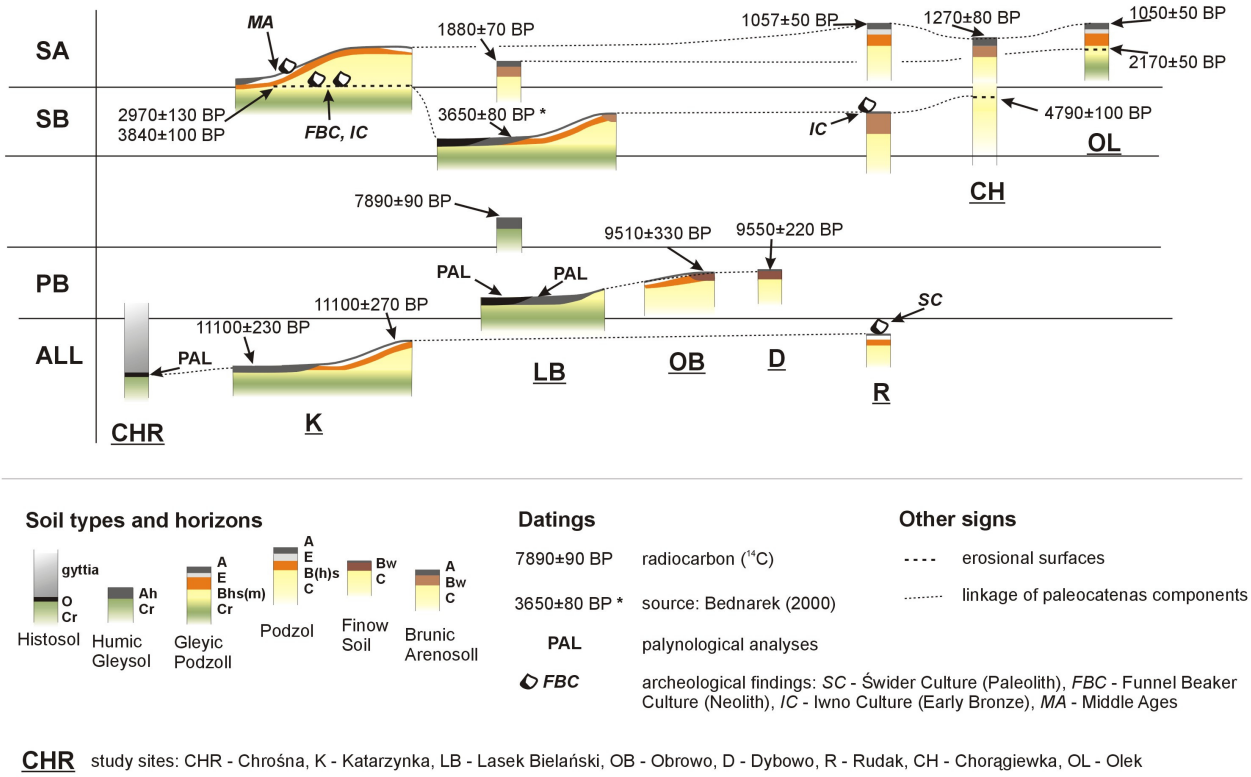

Figure 2. Combined chronosequence of soil paleocatenas in the dune area of the Toruń Basin in the light of ^{14}C, palynological and archaeological datings

Table 1. Fe_d/Fe_t ratio as an evidence of developmental stage of soils in different age paleocatenas

Soil generation	Podzols	Gleyic Podzols	Brunic Arenosols	Humic Gleysols
Neoholocene (SA)	**CH** E: 0.30 Bhs: 0.49	**K, Ol** E: 0.54-0.60 Bhs: 0.65-0.70	**LB** Bw: 0.28	-
Neoholocene (SB-SA)	**R** E: 0.54 Bs: 0.54	**LB** E: 0.32 Bhm: 0.39 BmA: 0.46	**LB, W*** Bw: 0.28-0.51	**LB*** Ah: 0.59
Eo-Mesoholocene (PB-SB)	-	**LB** BmA: 0.46 E: 0.38 Bhs: 0.17	**R** Bw: 0.51	**LB*** Ah: 0.31
Preboreal (PB)	**OB** (E): 0.29 (Bs): 0.27	**OB** (EA): 0.19 (Bs)Cr: 0.28	-	-
Alleröd (All)	**K** E: 0.20-0.37 Bs: 0.20-0.23	-	-	**K** Ah: 0.07

* - source: Bednarek (2000); **Ch** - symbols of study sites (see fig. 1); E, Bhs, Bhm, Bw, Cr, Ah – soil horizons symbols acc. To FAO (2006)

Despite of typological similarity, various age dune paleosols clearly differ in stage of development, depending on conditions and length of pedogenesis. This can be demonstrated by both, morphological and chemical properties (Table 1). Soils formed during Alleröd and in the first part of Preboreal period have shallow profiles, less distinct genetic horizons and low Fe_d/Fe_t ratios (0.1-0.4). Soil-forming processes have found the strongest expression in soils representing Eo-Mesoholocene and Neoholocene paleocatenas (Fe_d/Fe_t ratios: 0.3-0.7) .

Conclusions

Studies of toposequences and numerous single paleosols, carried out in the dune area of the Toruń Basin, allowed us to construct combined chronosequence of paleocatenas of four generations of soils, developed during: Alleröd, Preboreal, Eo-Mesoholocene and Neoholocene. Catenary variability of soil types reflects diversity of vegetation and the whole landscapes, during particular periods of pedogenesis. Time spans of soil development were separated by phases of aeolian activity, including wind erosion and burial of the former soil mantle. Although at the break of Late Glacial and Holocene, climate conditions were responsible for dune forming processes, human impact became the main driving force of aeolian activity initiation during Neoholocene.

References

Bednarek R (2000) Gleby kopalne jako źródło informacji o zmianach środowiska przyrodniczego. *Acta Universitatis Nicolai Copernici*, *Geografia* **31**, 47-63.

FAO (2006) 'Guidelines for soil description'. 4th edition, (Food and Agriculture Organization of the United Nations, Rome)

Jankowski M (2002) Buried soils in dunes of the Toruń Basin. In 'Paleopedology problems in Poland' (Eds B Manikowska, K Konecka-Betley, R Bednarek) pp. 233-252. (Łódzkie Towarzystwo Naukowe, Łódź)

Kaiser K, Barthelmes A, Czakó Pap S, Hilgers A, Janke W, Kuhn P, Theuerkauf M (2006) A Lateglacial palaeosol cover in the Altdarss area, southern Baltic Sea coast (northeast Germany): investigations on pedology, geochronology and botany. *Netherlands Journal of Geosciences* **85**, 3, 197-220.

Manikowska B (1991) Vistulian and Holocene aeolian activity, pedostratygraphy and relief evolution in Central Poland. *Zeitschrift für Geomorphologie N.F. Suppl.* **90**, 131-141.

Schirmer W (1999) Dune phases and soils in the European sand belt, *GeoArcheoRhein* **3**, 11-42.

Schlaak N (1993) Studie zur Landschaftsgenese im Raum Nordbarnim und Eberswalder Urstromtal. Berliner Geographische Arbeiten, 76.

Valentine KWG, Dalrymple JB (1975) The identification, lateral variation, and chronology of two buried paleocatenas at Woodhall Spa and West Runton, England. *Quaternary Research* **5**, 551-590.

Wilson P (1987) Pedogenic and geomorphic evolution of a buried dune palaeocatena at Magilligan Foreland, Northern Ireland. *Catena* **14**, 501-517.

Zeeberg J (1998) The European sand belt in eastern Europe - and comparison of Late Glacial dune orientation with GCM simulation results. *Boreas* **27**(2), 127-139.

Geographic relevance of Late Pleistocene and Middle Holocene aeolian deposits in Central Tuscany (Italy)

S.Priori[A] and E. A. C. Costantini [A]

[A]C.R.A.-A.B.P., Research Center of Agrobiology and Pedology, Firenze, Italy, Email priorisimone@gmail.com

Abstract
In central Italy, aeolian deposits of different nature are very scarce and often difficult to recognize. This paper reports the results of the work made by our research group during the last twenty years about the polygenetic paleosols with aeolian cover in the Elsa river basin (central Italy). During these studies we analyzed the texture, the chemical-physical parameters, the mineralogy, the micromorphology (soil thin sections and quartz grains exoscopy) and the geochemistry of the paleosols. In addition, we dated some horizons by OSL. The soil profiles with aeolian covers were located in stable landforms as dolines and karstic plateau. Therefore, limestone was the most common bedrock where the aeolian deposits were found, but we also found aeolian material on other lithologies, like Pliocene marine deposits and Pleistocene fluvial sediments. The aeolian covers were characterized by a high content of silt (> 50-60 %), a clear-wavy limit and a lithological discontinuity with the underlying buried paleosol. The research demonstrated that soil wind erosion and deposition of soil materials was accompanied to a large extent by water erosion and colluvial deposition during the Late Pleistocene and the Middle Holocene in the Elsa river basin.

Key Words
Loess, aeolian deposition, paleosols, OSL dating, Mediterranean

Introduction

The occurrence of aeolian deposits can be difficult to recognize when they have been mixed with other sediments and weathered, which is often the case in soils. Aeolian material can derive from either local or short-distance transport, from nearby continental sources, or from longer-distance hemispheric transport, as it is the case for Saharan dust. The difficulties in aeolian material identification result in the underestimation of spatial distribution of loess in soils, especially in Mediterranean Europe, where thick and uniform loess covers are rare, due to the limited extension of the alpine glaciations. In Italy, loess has only been reported for northern Italy and the Adriatic part of central Italy (Cremaschi 1990; Haase *et al.* 2007), with the Tosco-Emilian Apennine chain being regarded as a physiographic boundary of loess sedimentation (Cremaschi 1990). No loess has been described so far in the Tyrrhenian part of central Italy, but Pleistocene aeolian sand dunes have been reported by authors along the Tyrrhenian costs of central Italy (Cremaschi and Trombino 1998). The general aim of the research was to demonstrate the geographic relevance of the loess cover in Central Italy. The paper groups the experiences of twenty years of research work about paleosols of the Elsa river basin (Tyrrhenian side of Central Italy), so to delineate the areas with known aeolian cover.

Methods

The study area is located in central Tuscany (Central Italy) and it is mainly characterized by an eastern ridge (Chianti hills) formed by sedimentary rocks (Figure 1), a western ridge (Middle Tuscany Ridge) formed by metamorphic and sedimentary rocks, and a central ancient marine basin of the Pliocene period (4.8 - 4 My B.P.). The hills of the ridges are usually lower than 600-700 m s.l., whereas the hills formed in the marine deposits of the central basin are lower than 300-400 m s.l.

Previous studies (Mirabella *et al.* 1992; Costantini *et al.* 1996; Napoli *et al.* 2006; Priori *et al.* 2008) suggested the polygenetic nature of most of the soils formed in stable morphologies like dolines, plateau, terraces, and in some cases, lower part of footslopes. The beginning of pedogenesis of the most developed paleosols was estimated from the Early Pleistocene. The soils formed during this period were characterized by thick nitic horizons over the limestone, plinthite or ferrallitic horizons over the other bedrocks. Argic horizons, rubefaction, or ferric properties, were present in paleosols developed from the Middle Pleistocene - beginning of the Late Pleistocene. The soils younger than last interglacial (125 – 85 ky B.P.) usually showed cambic, vertic, calcic, mollic and thin argic horizons with moderate clay illuviation.

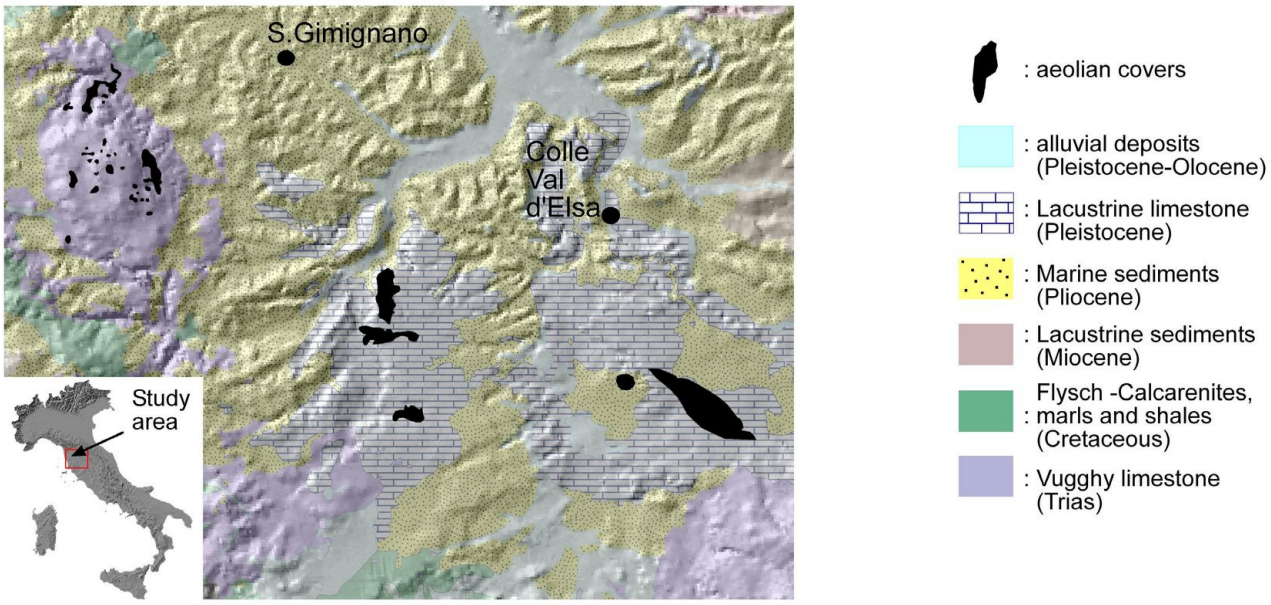

Figure 1. Geological map and aeolian covers of the study area.

Many surficial and sub-surficial horizons of the paleosols in the area had particle size classed in silt, were massive or poorly structured, and showed lithological discontinuities with the underlying argic and other more developed horizons. Priori et al. (2008) and Costantini et al. (2009) demonstrated that some or most part of these horizons formed from aeolian deposits. Some datings by OSL method (Costantini *et al.* 2009) reported an age from Late Pleistocene (about 70-60 ky B.P.) to Middle Holocene (3-5 ky B.P.). The aeolian nature of the parent material was checked by means of texture analysis, geochemistry and micromorhpology, both soil thin section and quartz grains exoscopy (SEM, Figure 4).

Results and discussions

The loess cover was characterized by the high silt content (> 50-60%, Figure 3) and the lithological discontinuity between the buried paleosols and the cover (Figure 2). The aeolian material was only widespread in stable surfaces (plateau, terraces) or natural morphological traps like dolines. The aeolian material was often mixed with colluvial material, gravels and pedorelicts. The texture of the aeolian covers was typically silt loam and silt clay loam, or silty clay. On the contrary, the textures of the buried paleosols varied from clay to clay loam and sandy loam. The thickness of the aeolian covers ranged from 0.20-0.30 to 1-1.5 m. The thickest covers were placed inside the dolines and were often mixed with colluvial material.

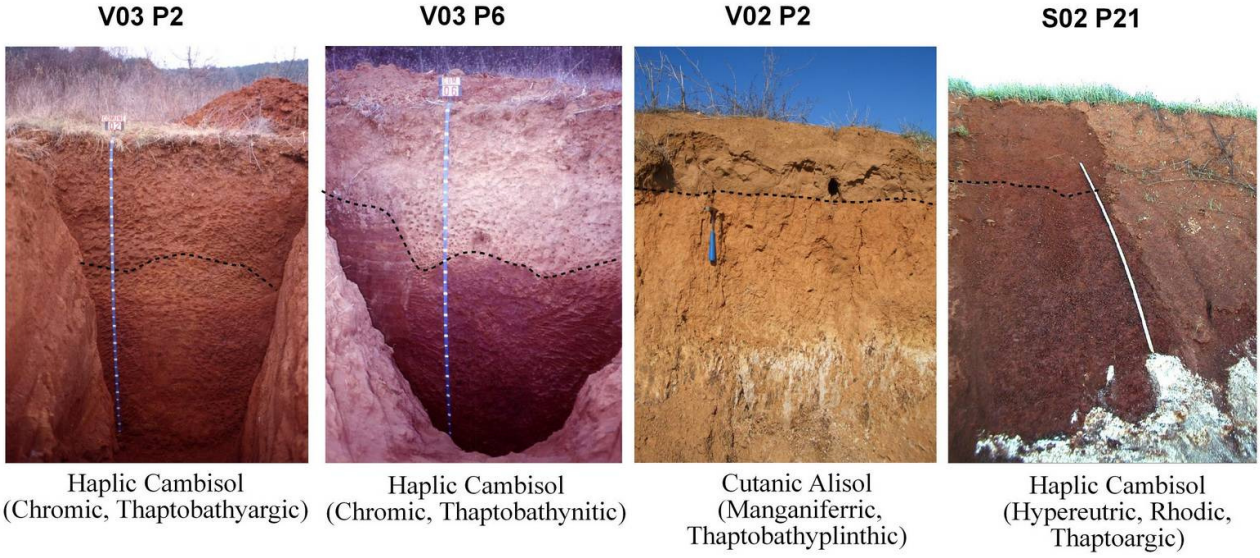

Figure 2. Four profiles with aeolian cover burying more strongly developed soil horizons (dotted line point to the boundary between the aeolian cover and the lower part of the paleosol).

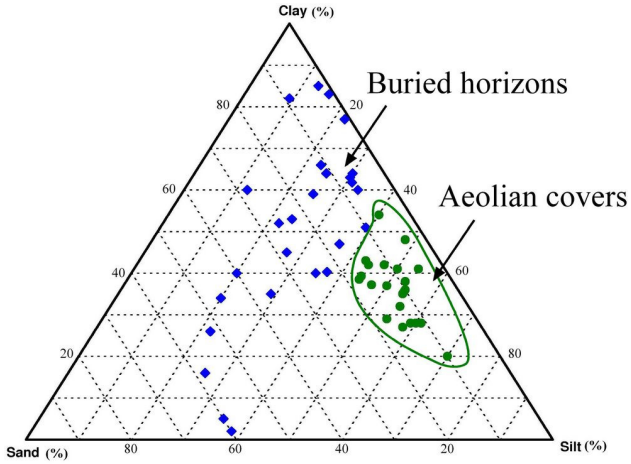

Figure 3. Textural ternary graph of the studied soils. The aeolian covers are grouped between the clay loam and the silt loam classes.

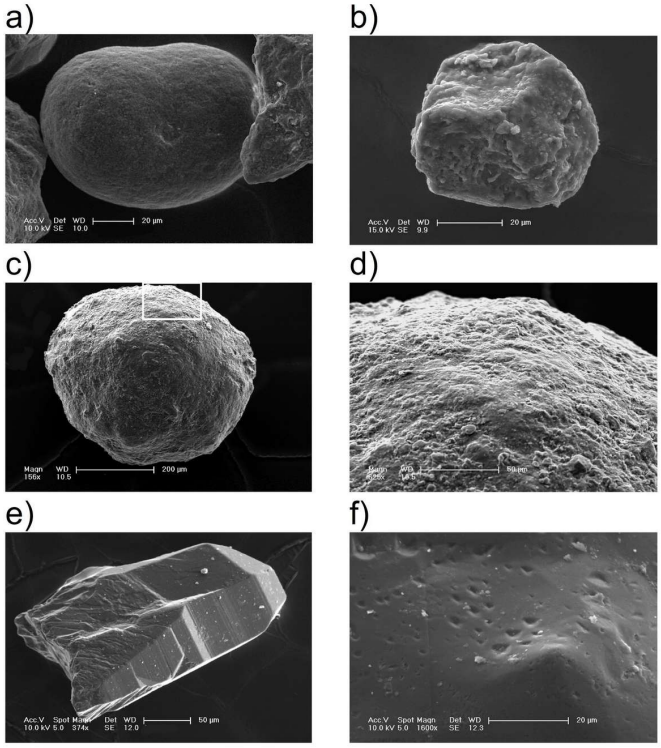

Figure 4. SEM images of quartz grains surfaces of aeolian covers (a,b,c,d) and buried paleosols (e,f). a) rounded coarse silt grain, b) sub-rounded grain with dish shaped concavities, c) rounded fine sand grain with "orange peel" surface, d) close-up of previous picture: upturned plates of silica, e) euhedral quartz grain with poorly smoothened corner, f) V-shaped holes.

The origin of the aeolian cover of the paleosols in the Elsa river basin is not homogeneous. Glacial or periglacial deposits however can be excluded, because there is no evidence of these processes, neither in the landforms, nor in the soils. Moreover volcanic ashes, although sometimes present in some soils, did not affect the bulk composition of the cover. Saharan dust as a major component can also be excluded, because the particle size of the cover is too coarse for an aeolian transport of more than several thousands of kilometres (Pye, 1995). The geochemistry of the covers permitted to attribute the source of the loess material to the alluvial fans and the wide alluvial plains of the rivers that drained the Middle Tuscany ridge and the Chianti hills (Costantini *et al.* 2009). During the driest stages of the Late Pleistocene and Holocene, these environments should have wide, bare and arid surfaces, strongly favourable for the aeolian erosion. The fluvial source of loess is reported in literature by Pye (1995), who called these deposits as "secondary loess", that is, loess redeposited and/or originated by other, non-eolian processes.

Conclusions

This paper demonstrates the presence of a loess cover on some polycyclic paleosols located in the Elsa river basin (Central Italy). The high content of silt of the cover and the clear, wavy limit with the underlying buried horizons, as well as the geomorphological position of the paleosols, helped in the identification of the loess in the field. The thickness of the loess cover, although sometimes affected by colluvial accumulation, was significant, which testifies that the process was not local, but geographically relevant, so to involve all the Elsa river basin, and possibly other areas of Central Italy. In conclusion, the research work demonstrated that soil wind erosion and deposition accompanied to a large extend water erosion and colluvial deposition during Late Pleistocene and Middle Holocene in the Elsa river basin. Although Central Italy is currently considered to be only marginally affected by wind soil erosion, a climatic change which would imply increased arid conditions could trigger a new cycle of slope denudation, wind erosion and loess deposition.

References

Costantini EAC, Napoli R, Bragato G (1996) Properties and geographic relevance of fragipan and other close-packed horizons in a non-glaciated Mediterranean region. *Geografia Fisica e Dinamica Quaternaria* **19,** 29-45.

Costantini EAC, Priori S, Urban B, Higers A, Sauer D, Protano G, Trombino L, H Hülle D, Nannoni F (2009) Multidisciplinary characterization of the middle Holocene eolian deposits of the Elsa river basin (central Italy). *Quaternary International* **200**, 107-130.

Cremaschi M (1990). 'The loess in northern and central Italy: a loess basin between the Alps and the Mediterranean region'. Quad. Geodinamica Alpina e Quaternaria 1. (Centro di Studio per la Stratigrafia e Petrografia delle Alpi Centrali: Milano).

Cremaschi M, Trombino L (1998) Eolianites, Sea level changes and Paleowinds in the Elba Island (Central Italy) during the Late Pleistocene. In 'Dust, aerosols, Loess Soil and Global changes'.(Ed AJ Busacca) pp. 131-134. (Washington State Univ. Coll. Of Agriculture and Home Economics: Pullman, WA)

Haase D, Fink J, Haase G, Ruske R, Pécsi M, Richter H, Altermann M, Jager KD (2007) Loess in Europe- its spatial distribution based on a European Loess Map, scale 1:2,500,000. *Quaternary Science Reviews* **26,** 1301–1312.

Mirabella A, Costantini EAC, Carnicelli S (1992) Genesis of a polycyclic Terra Rossa (Chromic Cambisol on Rhodic Nitisol) at the Poggio del Comune in Central Italy. *Zeitschrift für Planzenernahrung und Bodenkunde* **155**, 407-413.

Napoli R, Costantini EAC, D'Egidio G (2006) Using Pedostratigraphic Levels and a GIS to generate three-dimensional maps of the Quaternary soil cover and reconstruct the geomorphological development of the Montagnola Senese (central Italy). *Quaternary International* **156-157,** 167-175.

Priori S, Costantini EAC, Capezzuoli E, Protano G, Hilgers A, Sauer D, Sandrelli F (2008) Pedostratigraphy of Terra Rossa and Quaternary geological evolution of a lacustrine limestone plateau in central Italy. *Journal of Plant Nutrition and Soil Science* **171,** 1-15.

Pye K (1995) The nature, origin and accumulation of loess. *Quaternary Science Reviews* **14,** 653–667.

Geomorphic controls of biological soil crust distribution, Mojave Desert (USA)

Amanda Williams[A], Brenda Buck[B], Debbie Soukup[C], Douglas Merkler[D]

[A]Ph.D. Student, Department of Geoscience, University of Nevada, Las Vegas, USA, Email willamje@unlv.nevada.edu
[B]Faculty, Department of Geoscience, University of Nevada, Las Vegas, USA, Email buckb@unlv.nevada.edu
[C]Faculty, Department of Geoscience, University of Nevada, Las Vegas, USA, Email gsoukup@bak.rr.com
[D]Resource Soil Scientist, NRCS, USDA, Las Vegas Field Office, USA, Email Doug.Merkler@nv.usda.gov

Abstract
Biological soil crusts (BSCs) are vital features of arid regions. These crusts form living skin that mitigates erosion, influences soil fertility, manages soil moisture/temperature, and prevents desertification. BSCs are fragile resources, easily destroyed by physical disturbances and potentially impacted by climate change. Our investigation employs a novel, interdisciplinary approach to investigate BSC biotic potential (bridging gaps among biology, ecology, soils, hydrology, statistics, chemistry, geomorphology, remote sensing, and GIS).

Our study documents important links among BSCs, soils, geomorphology, and land stability. Results indicate geomorphic stability and dust influx impact BSC composition and development. Soil stability ultimately controls biotic potential of cyanobacterial versus moss-lichen crust; however, dust influences both crust types through texturally enhanced water-holding capacity and increased soil fertility. Soil chemistry of moss-lichen substrates exhibit a potential dust signature, with elevated Ca, K, Mg, B, Fe, Ni, Co, Mn, Cl, and EC. While results indicate inherent geomorphic stability controls BSC development, we suggest BSCs enhance their propagation through dust capture and erosion mitigation. These soil-geomorphic relationships present insight into arid landscape evolution, providing tools to improve BSC mapping and land management.

Key Words
biological soil crust, ecology, pedogenesis, geomorphology, erosion, dust

Introduction

Biological soil crusts (BSCs) provide critical ecosystem services in deserts around the world. These crusts are microbial complexes that fuse around soil particles to create a living, protective skin. BSCs fill plant interspaces, covering up to 70 percent of the landscape (Friedmann and Galun 1974; Belnap 1994; Belnap 1995). BSCs improve soil productivity and desertification resistance by impacting soil erosion/deposition, water movement, energy balances, landscape stability, soil fertility, and plant community establishment (Eldridge and Greene 1994; Belnap 1995; Belnap *et al*. 2001).

BSCs are easily destroyed by physical impacts (off-road vehicles, hiking, grazing, etc.), making them highly sensitive to land use changes (Belnap 1995). BSCs present unique challenges to land managers (Belnap et al., 2001). The organisms' size and patchy growth make large-scale mapping and modelling impractical (Eldridge and Rosentreter 1999; Belnap et al. 2001). Furthermore, the ecological controls of BSC distribution are poorly constrained, particularly within the Mojave Desert (USA). In this study, we investigated the complex interrelationships between BSCs and soil-geomorphology to address ecological questions and mapping challenges.

Methods

Soil-geomorphology data were compared and contrasted with BSC data. Eleven BSC units (plus sandstone/limestone outcrops and roads) were delineated and described according to species composition and surface characteristics. Ten geomorphic surfaces were mapped according to topography, elevation, depositional environment, and soil profile development (as seen along washes). Units included alluvium (10 units with ages ranging from Late Miocene/Earliest Pleistocene to recent Holocene), active sand sheets, colluvial slopes, limestone, sandstone, and roads. A soils map was derived through correlation of USDA Official Soil Series with geomorphic units (Soil Survey Staff 2007). Seven soil units were successfully correlated with four series (Arizo, Bluepoint, Ferrogold, Irongold)(Soil Survey Staff 2007). Uncorrelated soils were named according to their taxonomy (Soil Survey Staff, 2006). Soil and geomorphic maps were overlayed with the BSC map for percent overlap between map units (ESRI Arc GIS 9.2 Desktop; Microsoft Excel). Transect data were collected from 36 plots to quantify soil cover and environmental characteristics within BSC map units. BSC samples were microscopically analysed to confirm genera identification. Surface soils were sampled and analysed for soil texture, pH, EC, total C, inorganic C, organic C, total N, NO_3, total S, SO_4, Cl, PO_4, K, Ca, Fe, Mg, B, Mn,

Cu, Zn, Mo, and Ni. Data were statistically analysed with Pearson product-moment correlation coefficients (Microsoft Excel) and multivariate statistical techniques including Nonmetric Multidimensional Scaling (NMS) and Multiresponse Permutation Procedures (MRPP) (MJM Software 2006).

Results

Soils & Geomorphology

Overlays between BSCs and soil/geomorphic maps revealed high correlation between cyanobacterial crusts and sand sheets. The cyanobacterial-dominated BSC unit had 66% overlap with geomorphic unit "Qe" and soil series "Bluepoint". These sand sheet units are >1m deep with negligible soil development. Moss-lichen crusts were correlated with mid-Holocene alluvial soils. Pinnacled BSC units overlapped 57-59% with geomorphic units "Qay_1"and "Qay_2" and overlapped 57-59% with "Arizo" soil series. These surfaces have sandy-skeletal soils with Stage I-II carbonate morphology, incipient Av horizon development (within moss-lichen pinnacles), and faint bar and swale morphology. Transect data yielded similar results, with high-moss lichen cover on Arizo soils and geomorphic surfaces $Qay_1$and Qay_2; while high cyanobacterial cover was found on Bluepoint soils and Qe geomorphic units.

Ecology

Pearson product-moment correlations of interspace cover versus environmental characteristics are summarized in Table 1. Multiple environmental variables were overlayed on a three-dimensional NMS ordination. Environmental factors accounted for 92% of the variability found in interspace BSC distribution.

Interspace Characteri-stics	% Interspace Cover		
	Cyano-bacteria	Moss & Lichen	Total BSCs
% Limestone	-0.49	-0.47	-0.80
Rock Cover	-0.57	-0.43	-0.83
% Bare	0.38	-0.39	-0.08
% Bromus Rubens	-0.21	0.27	0.09
Pleuraphis rigida	0.61	-0.22	0.25
Hymenoclea salsola	-0.26	-0.11	-0.30
Larrea Tridentata	0.51	0.01	0.39
Eriogonum fasciculatum	-0.06	0.29	0.22
Max. Pinnacle Ht.	-0.15	0.73	0.55
% Clay	0.33	-0.40	-0.12
% Silt	-0.29	-0.01	-0.23
% VF Sand	-0.20	0.38	0.19
% F Sand	0.34	0.00	0.26
K	-0.22	0.55	0.34
Mg	-0.06	0.55	0.46
Ca	-0.41	0.61	0.26
Cl	0.16	0.19	0.30
SO_4	-0.21	0.07	-0.09

Interspace Characteri-stics	% Interspace Cover		
	Cyano-bacteria	Moss & Lichen	Total BSCs
NO_3	-0.16	-.010	-.021
Mn	0.12	0.30	0.37
Fe	-0.29	0.47	0.22
Ni	-0.25	0.48	0.25
Cu	0.23	-0.53	-0.32
Co	0.06	0.30	0.33
B	-0.35	0.61	0.30
Mo	0.33	-0.15	0.12
Available P	-0.41	0.18	-0.15
pH	0.03	-0.40	-0.35
EC	-0.30	0.55	0.28
Total C	-0.57	-0.07	-0.50
Inorg. C	-0.52	-0.20	-0.58
Org. C	-0.44	0.05	-0.29
Total N	-0.43	0.26	-0.08
Total S	-0.12	0.27	0.16
C:N Ratio	-0.39	-0.33	-0.60
Carbonate	-0.52	-0.20	-0.58

$R^2 > 0.39$

$R^2 < -0.39$

$R^2 > 0.19$

$R^2 < -0.19$

Table 1. Pearson's product-moment correlation coefficients (R^2) are summarized for selected interspace characteristics. Results are reported as correlations between percent interspace cover and other characteristics.

An NMS plot (Figure 1) illustrates select correlations among biological and environmental variables. NMS analyses show lichen, moss, and grass (invasive *Bromus rubens*) are all positively associated with K, B, Ca, EC, Fe, very fine sand, and pinnacle relief and are negatively associated with cyanobacteria cover and bare soil. BSC cover classes (moss, lichen, and cyanobacteria) are negatively associated with limestone cover, NO_3, C:N ratios, inorganic carbon (carbonate), and Cu.

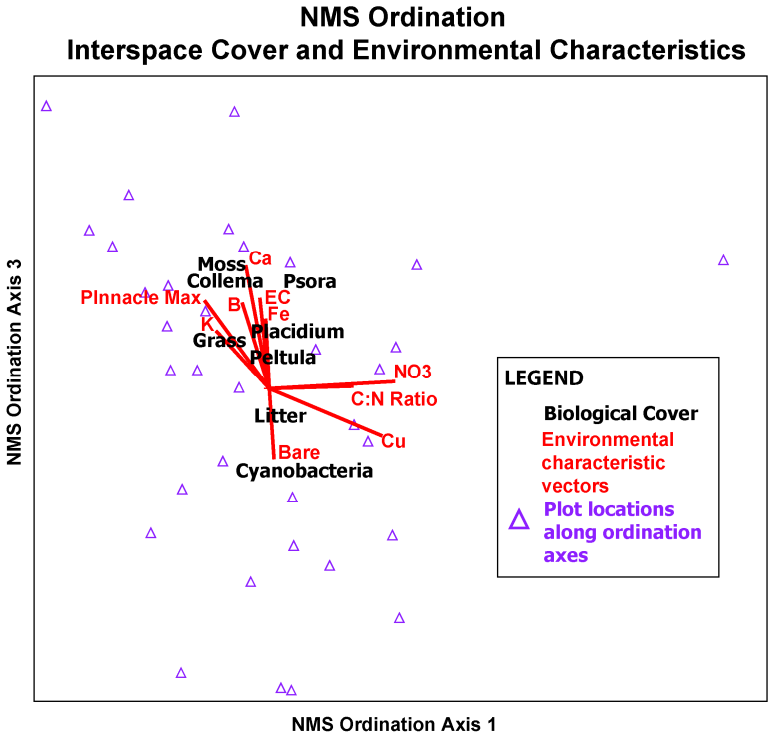

Figure 1. A 3-D NMS ordination of soil interspace shows relationships among biological variables (2-D shown). Strongly associated species (in black) are shown closer together. Plots (triangles) are graphed closest to their compositional species. Red lines (vectors) point to species with which they are strongly associated.

MRPP analyses tested the effectiveness of soil, geomorphic, and BSC map units in grouping interspace cover. MRPP results are reported as association values (A). When A=1, group members are identical; and when A=0, group members are not similar (McCune and Grace, 2002). McCune and Grace (2002) state A>0.3 are high values for ecological data sets. MRPP results showed the following: soil map units (A=0.29; p=0.00000875), BSC map units (A=0.52; p=0.00000000), geomorphic map units (A=0.35; p=0.00000657).

Discussion

Soils and Geomorphology

Results indicate a strong relationship between soil-geomorphology and BSC distribution. Cyanobacteria crusts are most prominent on surfaces of high geomorphic instability, namely sand sheets. Instability only permits establishment of mobile BSC organisms, such as *Microcoleus sp*. Moss-lichen crusts are most extensive on stable surfaces with maximum dust influx, specifically mid-Holocene surfaces. These surfaces are elevated from active alluvial processes, but have increased surface roughness compared to older geomorphic surfaces and therefore receive higher rates of dust accumulation (McFadden et al., 1987). Dust enhances the water-holding capacity and fertility of the soil, thereby improving BSC growth and development. Moss-lichen BSCs may amplify the dust capture along mid-Holocene surfaces by increasing microtopography and decreasing erosional losses. These positive feedback mechanisms may allow BSCs to effectively "engineer" their habitat to improve propagation. MRPP analyses suggest soil and geomorphic maps are effective predictors of BSC distribution, greatly enhancing ecological crust models.

Ecology

Results show BSC distribution is strongly influenced by dust-related texture and chemistry changes. Cyanobacterial crusts are highly correlated with clay volumes, perhaps because their sticky sheaths capture the finest dust fraction. Microscopic observations of cyanobacteria confirmed presence of soil fines in extracellular polysaccharides. Moss-lichen crusts are associated with the very fine sands, likely derived from the coarser dust fraction. In both cases, dust influx increases the concentration of fine particles, enhancing soil water-holding capacity, soil fertility, and BSC propagation.

Soil chemistry of moss-lichen substrates suggests an influence of dust, with elevated concentrations of Ca, K, Mg, B, Fe, Ni, Co, Mn, Cl, and high EC. Depending on the source area, dust may contain high levels of macro- and micronutrients beneficial to BSC growth. In contrast, Cu is negatively correlated with moss-lichen cover.

While it is unclear why Cu relationships differ from those of other metallic ions, we hypothesize that some organic chelator (associated with BSCs) may increase its mobility. Alternatively, BSC organisms may be hyperaccumulating copper, but one would expect turnover to offset uptake.

Nitrate (NO_3) is negatively correlated with moss-lichen crusts, with low nitrate levels under moss-lichen relative to soil below rock fragments. Organic matter from pinnacled BSCs may increase the time soils remain moist. If so, net denitrification would be higher below moss-lichen BSCs, explaining nitrate losses. Likewise, extensive rock cover could increase runoff and decrease infiltration, lowering soil moisture and net denitrification relative to soils under BSCs. The source of nitrate is likely salt-rich dust fall, as nitrate, sulfate, and chloride are all positively correlated with each other. Total nitrogen is positively correlated with moss-lichen cover. BSC tissues found in soil samples may account for additional nitrogen. The nitrogen budget of this system warrants further investigation.

Conclusions

This study illustrates the importance of soil-geomorphic characteristics in controlling BSC distribution. While geomorphic processes largely control surface dynamics, our results suggest BSCs also play an active role in soil stabilization and dust trapping. Dust accumulation strongly influences surface soil chemistry with elevated concentrations of clays/fine sands, Ca, K, Mg, B, Fe, Ni, Co, Mn, Cl and high EC associated with moss-lichen substrates. In contrast, NO_3 and Cu are both negatively correlated with BSCs. Moss-lichen crusts could have greater soil moisture leading to higher net denitrification. Organic chelators associated with moss and lichen could lead to increased Cu mobility. These important connections between soil-geomorphic characteristics and crusts highlight the potential use of surficial mapping in BSC management. While current efforts examine moisture availability impacts in crust growth, continued research will explore the complex role of BSCs in soil landscape evolution through time.

References

Belnap J (1994) Potential role of cryptobiotic soil crust in semiarid rangelands. In 'Proceedings – Ecology and Management of Annual Rangelands'. (Ed SB Monsen, SG Kitchen S.G) pp. 179-185. (USDA Forest Service, Intermountain Research Station: Ogden, UT).

Belnap J (1995) Surface disturbances: their role in accelerating desertification. *Environmental Monitoring and Assessment* **37**, 39-57.

Belnap J, Kaltenecker J, Rosentreter R, Williams J, Leonard S, Eldridge D (2001) 'Biological Soil Crusts: Ecology and Management'. Technical Reference 1730-2. (U.S. Department of the Interior: Denver, CO).

Bowker MA, Belnap J, Davidson DW, Goldstein H (2006) Correlates of biological soil crust abundance across a continuum of spatial scales: support for a hierarchical conceptual model. *Journal of Applied Ecology* **43**, 152-163.

Eldridge DJ, Greene RSB (1994) Microbiotic soil crusts: A review of their roles in soil and ecological processes in the rangelands of Australia. *Australian Journal of Soil Research* **32,** 389-415.

Eldridge DJ, Rosentreter R (1999) Morphological groups: a framework for monitoring microphytic crusts in arid landscapes. *Journal of Arid Environments* **41**, 11-25.

Friedmann EI, Galun M (1974) Desert algae, lichens and fungi. In 'Desert Biology". (Ed. GW Brown) pp. 165-212. (Academic Press, New York).

McCune B, Grace JB (2006) 'Analysis of Ecological Communities, 2nd ed'. 304 pp. (MjM Software: Gleneden Beach, Oregon, USA).

McFadden LD, Wells SG, Jercinovich MJ (1987) Influences of eolian and pedogenic processes on the origin and evolution of desert pavements. *Geology* **15,** pp. 504-508.

MJM Software (2006) PC-ORD™, v5. (MjM Software: Gleneden Beach, Oregon, USA).

Soil Survey Staff (2006) 'Keys to Soil Taxonomy, 10th ed.' (USDA-Natural Resources Conservation Service: Washington, DC).

Soil Survey Staff (2007) "Soil survey of the Clark County area, NV'. (Natural Resources Conservation Service: Washington, D.C.). http://soildatamart.nrcs.usda.gov/Survey.aspx?State.

Glacial dust in soils of Pennsylvania, USA: Evidence for an eolian component of fragipan horizons

Katherine Lindeburg[A], Patrick Drohan[B], William Waltman[C], Austin Young[D], Mary Kay Lupton[E]

[A]Graduate student of Crop and Soil Sciences, Pennsylvania State University, University Park, PA, USA, Email ksl149@psu.edu
[B]Faculty of Crop and Soil Sciences, Pennsylvania State University, University Park, PA, USA, Email pjd7@psu.edu
[C]Educator of Horticulture and Agriculture, Pennsylvania State Coop. Extension, Coudersport, PA, USA, Email wjw15@psu.edu
[D]Staff of Crop and Soil Science, Pennsylvania State University, University Park, PA, USA, Email mxk397@psu.edu
[E]Student of Crop and Soil Science, Pennsylvania State University, University Park, PA, USA, Email aay5003@psu.edu

Abstract
Contributions of glacial dust (loess) to soils that result in a loess parent material and subsequent soil profiles imprint a unique geochemical signature and profile morphology. In areas where loess deposits are thinner, capping a differing parent material, or perhaps re-worked over time, identifying such polygenetic soils becomes more difficult. In this paper, we present preliminary results of a larger study of eolian additions to Pennsylvania soils and compare soils with fragipan subsoil horizons derived from pre-Wisconsinan and Wisconsinan glacial tills. Preliminary results suggest widespread eolian additions across both glacial periods, dust incorporation into parent materials of both soils prior to its formation, and dust inputs following fragipan formation. We suggest a general chronology of fragipan formation and degradation that explains the incorporation of loess into the soil profiles.

Key Words
Appalachians, pedogenesis, mineral aerosols, aeolian deposition

Introduction
The extent of wind-blown (eolian) surface additions to non-loessal soils is poorly documented for much of the Northeastern United States (N.E.U.S.). In the N.E.U.S., eolian deposits associated with the last glacial maximum (LGM) have assumed to be small, based on General Circulation Model (AGCMs) predictions of anticyclonic circulation and winds from the east and northeast (COHMAP Members 1988) and large distances from the Midwestern source regions. In contrast, patterns of loess distribution in the midcontinent and recent simulations of prevailing paleowinds from the west and north-west during last glacial period (Bettis III *et al.* 2003; Muhs and Bettis III 2000) suggest conditions conducive to dust transport from local sources and regional redistribution. Such paleoclimatic models are consistent with loess sequences in Pennsylvania (Carey 1978; Millette 1955) and observations of regional eolian deposits. Anomalously high silt contents in limestone and dolomite valleys (Cronce 1987), colluvial surface soils in the Ridge and Valley (Ciolkosz *et al.* 1986; Peterson *et al.* 1970), footslope colluvium (Hoover 1983), and ridge tops (Ciolkosz *et al.* 1990) have been attributed to widespread eolian deposition and interpreted alongside additional evidence for significant geomorphic alteration of unglaciated landscapes during glacial periods (Ciolkosz *et al.* 1986).

Background and overview
The site-specific, but limited evidence of thin loess deposition across the N.E.U.S. requires further documentation. A potential mechanism to evaluate the regional influence of loess to soils would be to tie loess deposition to a landscape feature also believed derived contemporaneously with loess deposition. If such a feature was found to have a loess signature, then the regional extent of such thinner loess deposits would allow for much greater precision in mapping loess deposition. The fragipan subsoil horizon is potentially such a signature feature. The origin of the fragipan is still a matter of debate (Smalley and Davin 1982, and references therein). At the centre of this debate are the origins of its silt rich content, density, brittleness, and prismatic structure, which generally are attributed to pedogenic (e.g., shrink-swell cycles; clay illuviation) (Carlisle 1954; Jha and Cline 1963) or geogenic (e.g., density inherited from parent material; rapid desiccation, collapse, and crack formation) (Assallay *et al.* 1998; Bryant 1989) processes. If geogenic, than the fragipan's polygonal structure and density are largely a relict feature of landscape instability, and likely derived at the end of a glacial event when loess deposition is typically widespread. Landscape movement of a moist to wet colluvial deposit, with loess incorporated during movement, resulted in eventual settling and desiccation of a silt rich horizon; settling and desiccation produced prisms and particle contraction enhancing density increases in the fragipan.

Research on chronosequences of soils with fragipans has shown that fragipan aging is associated with a reduction of prism circumference, increased distance between prism centres, reduction of prism bulk density, and an increased differentiation with depth in fragipan prism and face material (Waltman 1981). These observations suggest a mechanism for fragipan degradation over the course of pedogenesis and provide reasonable support that, to some degree, crack growth and infilling occur because of and alongside prism degradation. Nevertheless, explanations of how observed differences in particle size, mineralogy, and geochemistry of prism matrix and faces were derived in pedologically old soils are not entirely agreed upon.

Objectives of this study are (1) to evaluate the extent and spatial distribution of eolian materials in glacial till soils across time, and (2) to evaluate whether fragipan is largely a relict subsoil feature. We address the first objective and test our first main hypothesis—namely, that till parent materials of soils and their fragipans were augmented with glacial dust—with silt mineralogy and particle shape, morphology, and surface features of fine and very fine sands. We base this approach on others' observations that mineralogy, shape parameters, and geochemistry are useful in sourcing sediments (e.g., Muhs and Bettis III 2000) because (a) mineralogy of local sediments may be distinct from hypothesized exotic sources, and hence, mineralogy can fingerprint distinct sources; (b) particle shape and morphology of glacial and eolian transport mechanisms are distinct from each other (Krinsley and Doornkamp 1973); and (c) features of (a) and (b) are maintained over course of pedogenesis. Essentially, the mineralogical and/or particle morphological alterations due to pedogenesis can be distinguished as such and differentiated from original parent properties.

To test our second main hypothesis—namely, that formation of prismatic structural units and inter-prism cracks was contemporaneous with till parent material deposition and rapid desiccation—we infer timing of parent material deposition and crack initiation from extent and distribution of an eolian component within the soils. Dust provides a temporal constraint on parent material deposition, and possibly also, on timing of crack initiation and origin of its polygonal structure because (a) eolian deposition is temporally constrained by paleoclimatic conditions (glacial periods), and Holocene deposition can be assumed negligible; (b) spatial distribution (matrix vs. face and depth trends) of dust reflects original deposition rather than reorganization during pedogenesis; and thus, is interpretable within a temporal and mechanistic fragipan formation model.

Methods

Study sites

We selected representative fragipan soils of central Pennsylvania developed from tills of similar lithology but different ages (Waltman 1981). Parent material of a pedologically old soil (coarse-loamy, mixed, mesic Aeric Fragiaquult) is the pre-Wisconsinan (>70,000 YBP) White Deer till, comprised of siltstone, conglomerate, and minor amounts of limestone; a pedologically young soil (fine-loamy, mixed, mesic Aeric Fragiaquept) developed from Wisconsinan (12,500 to 15,000 YBP) Woodfordian till, comprised of gray siltstone, shale, and sandstone.

Soil characterization

Analyses were made on subsamples of archived fine-earth (< 2-mm) soil samples (Waltman 1981). Concentrations of major, minor, trace, and rare earth elements (REEs) were determined by lithium metaborate fusion and elemental analysis by X-ray fluorescence (XRF) at ALS Chemex (Sparks, NV). Sand and silt particle size fractions were isolated for particle morphological and mineralogical analyses according to standard techniques (Soil Survey Staff 2004). Fine sand (250 to 125 μm) and very fine sand (125 to 50 μm) fractions were separated through wet sieving of dispersed samples following organic matter removal. Grain shape, morphology, and surface features were characterized using grain mounts of fine and very fine sand particle size fractions viewed with a petrographic microscope and scanning electron microscopy (SEM). Particle shape analyses were performed using ImageJ freeware. Mineralogy was determined for random powder mounts of silt fractions (50-10 μm and 10-2 μm fractions) using X-ray diffraction (XRD) Jade software. Statistical analyses were computed using Minitab Inc.

Results

Particle shape and surface morphology

Fine and very fine sands are generally more angular and less round in the Wisconsinan than those in the pre-Wisconsinan soil. In the Wisconsinan fragipan horizons, matrix and faces have statistically indistinguishable sand shape factors. In contrast, within the pre-Wisconsinan fragipan horizons, matrix sands are significantly less angular, more round, and have a greater solidity index than the face sands (p-value <0.05).

Particle size distribution and mineralogy
In both soils, fragipan matrix soils have more clay than fragipan faces and non-fragic soils. Non-fragic soils have significantly (p-value <0.05) more coarse silts and less medium and fine sands than fragipan soils. In the pedologically old pre-Wisconsinan soil, an abrupt increase in sand and decrease in silt occurs with depth at the boundary between the non-fragic horizons (Ap, E, and Bw) and the fragipan horizons below 56 cm.

Plagioclase and K-feldspar are dominant minerals comprising ~40% of the silt fraction of surface soils, and decline with depth to ~15% in the pedologically young Wisconsinan soil. In contrast, feldspars in the pre-Wisconsinan profile are only minor, if at all, mineral constituents of silts. Interestingly, while essentially absent below 56 cm, both plagioclase and K-feldspars are present—albeit, in minor amounts—in the shallowest soils (Ap, E, and Bw horizons) in the pedologically old pre-Wisconsinan profile.

Elemental composition
The pre-Wisconsinan and Wisconsinan soils exhibit similar, systematic differences in major and minor, trace, and REEs in fragipan matrix and faces. Faces are consistently enriched relative to matrixes in Si, Zr, and Ti; faces are depleted in Al, Fe, Mg, Ca, Na, K, Mn, and P. Between pedons, the pre-Wisconsinan has more Si and less Mg, Ca, Na, K, Mn, P, and Ti than the Wisconsinan soil. Differences within the Wisconsinan are restricted to lateral gradients between matrix and faces of fragipans. In contrast, systematic depth trends occur in addition to lateral differences in geochemistry of pre-Wisconsinan fragipan matrix and faces. Distinct changes in normalized and absolute concentrations of REEs and immobile elements and abrupt decline in base cations below 56 cm suggest that the Ap, Bt1, Bt2, and IIBx1 horizons are dissimilar in origin than soils below, and likely, reflects lithologic discontinuity within the pre-Wisconsinan soil.

Discussion
The differences in physical properties and mineralogy within the Wisconsinan soil result from pedogenic processes during ~15 ky of development. Dominant soil forming processes include weathering of primary minerals of low stability, losses of elements associated with the weatherable primary minerals, residual enrichment of resistant minerals and associated elements, production of secondary minerals, and translocation out of colloids from zones of weathering to zones and accumulation at depth. The minor differences in particle shape metrics and surface morphological properties likely are due to pedogenesis rather than a difference in material provenance: Matrix sands are subtly rounder than face sands, though, from SEM analyses, we interpret a similar origin of angular particles for the matrix and faces, and the explain the observed differences by pedogenic processes (preferential destruction or masking of matrix sand angularity from amorphous siliceous surface coatings). Results from elemental analyses and REEs corroborate our interpretations of particle shape and SEM analyses, providing further support for the same original parent source of fragipan face and fragipan matrixes.

In contrast, differences within the pre-Wisconsinan soil suggest a complex formation history in which pedogenic processes may have been augmented with or replaced by geomorphic alteration during periods of environmental conditions different than those of the present. The older soil exhibits differences between the matrix and face sand grain features which could reflect effects of spatial heterogeneity of weathering intensity within the fragipan or relatively recent additions of mineral dust. The presence of feldspars in the upper, non-fragic soil horizons may reflect a period of eolian deposition and incorporation into the soil long after the initiation of pedogenesis and crack formation. Surface soils and face material of the shallowest fragipan horizon are all enriched in Zr and REEs relative to deeper soils; without exogenous additions, we would expect the depletion at the surface and a decline in depletion with depth. Geochemical and mineralogical results corroborate soil textural clues to a lithologic discontinuity below the first fragipan horizon and support a polygenetic model of soil formation in the pre-Wisconsinan soil.

Conclusion
The particle shape matrixes and angular surface features observed in both pedons from SEM and particle shape analyses are compatible with modeled origin as glacial sediment and redistribution following wind-transport and deposition either locally or within a moderate proximity from the original sediment source (Krinsley and Doornkamp 1973; Pye 1995). Nevertheless, we recognize the potential origin of sand angularity from solely glacial processes without eolian transport and thus, focus our current research efforts on distinguishing between the two transportation mechanisms.

References

Assallay AM, Jefferson I, Rogers CDF, Smalley IJ (1998) Fragipan formation in loess soils: Development of the Bryant hydroconsolidation hypothesis. *Geoderma* **83**, 1-16.

Bettis III EA, Muhs DR, Roberts HM, Wintle AG (2003) Last glacial loess in the coterminous USA. *Quaternary Science Reviews* **22**, 1907-1946.

Bryant RB (1989) Physical processes of fragipan formation. *Soil Sci. Soc. Am. J.* **24**, 141-150.

Carey JB (1978) The genesis and morphology of four soils developed in loess. Ph.D. diss., Pennsylvania State University.

Carlisle FJ (1954) Characteristics of soils with fragipans in a Podzol region. Ph.D. diss., Cornell University.

Ciolkosz EJ, Carter BJ, Hoover MT, Cronce RC, Waltman WJ, Dobos RR (1990) Genesis of soils and landscapes in the Ridge and Valley Province of central Pennsylvania. *Geomorphology* **3**, 245-261.

Ciolkosz EJ, Cronce RC, Sevon WD (1986) Periglacial features in Pennsylvania. Pennsylvania State University, Agronomy Series No. 92, University Park, PA.

COHMAP Members (1988) Climate changes of the last 18,000 years: Observations and model simulations. *Science* **241**, 1043-1052.

Cronce RC (1987) The genesis of soils overlying dolomite in the Nittany Valley of central Pennsylvania. Ph.D. diss., Pennsylvania State University.

Hoover MT (1983) Soil development in colluvium in footslope positions in the Ridge and Valley Physiographic Province of Pennsylvania. Ph.D. diss., Pennsylvania State University.

Jha PP, Cline MG (1963) Morphology and genesis of a Sol Brun Acide with fragipan in uniform silty material. *Soil Sci. Soc. Am. Proc.* **591**, 339-344.

Krinsley DH, Doornkamp JC (1973) 'Atlas of quartz sand surface textures.' (Cambridge University Press: London).

Millette JFG (1955) Loess and loess-like deposits of the Susquehanna River Valley of Pennsylvania and a section of the Laurentians in Canada. Ph.D. diss., Pennsylvania State University.

Muhs DR, Bettis III EA (2000) Geochemical variations in Peoria Loess of western Iowa indicate paleowinds of midcontinental North America during last glaciation. *Quaternary Research* **53**, 49-61.

Petersen GW, Ranney RW, Cunningham RL, Matelski RP (1970) Fragipans in Pennsylvania soils: A statistical study of laboratory data. *Soil Sci. Soc. Am. Proc.* **34**, 719-722.

Pye K (1995) The nature, origin and accumulation of loess. *Quaternary Science Reviews* **14**, 653-667.

Smalley IJ, Davin JE (1982) Fragipan horizons in soils: A bibliographic study and review of some of the hard layers in loess and other materials. In 'New Zealand Soil Bureau Bibliographic Report 30'. (Department of Scientific and Industrial Research: Wellington, New Zealand).

Soil Survey Staff (2004) Soil survey laboratory methods manual. (U.S. Gov. Print. Office: Washington, DC).

Waltman WJ (1981) Fragipan morphology in late Wisconsinan and pre-Wisconsinan age soils of Pennsylvania. M.S. thesis, Pennsylvania State University.

Impact of aeolian sediments on pedogenesis – examples from the fringe area of the Saharan desert

Reinhold Jahn

Institute of Agricultural and Nutritional Sciences – Soil Sciences, University of Halle, Germany,
Email: reinhold.jahn@landw.uni-halle.de

Abstract
A series of soils was studied along a moisture gradient from the centre to the outer fringe area of the Saharan desert. The contribution of added aeolian material to the soils in general decreases along the moisture gradient but shows differences from the trend according to the age of the soils and the underlying rocks. The impact of the pedogenetic processes of soil horizon formation, accumulation of organic matter, carbonatisation, texture development and development of mineral assemblage is discussed. Also related consequences like changes in water storage capacity and ped formation are discussed according to their impact on pedogenesis. In general the impact on pedogenesis is not only a function of the amount of added materials, it differs also according to the properties of the specific soil material from a certain rock and the stage of soil development.

Key Words
Aeolian materials, pedogenesis, organic matter, carbonatisation, texture development

Introduction

All deserts are known as important source regions for aeolian dust. Early studies (Yaalon & Ganor, 1973; Péwé, 1982; Ganor & Mamane, 1982) resulted in estimates of 250 Mio. to more than 700 Mio. tons loss of materials per year (Figure 1). The deposition of aeolian dust is widely recognized as an important modifying part of soils. The rates of dust deposition observed across the globe vary from almost 0 to greater than 450 g m^{-2} yr^{-1} (Lawrence & Neff 2009). Sites receiving dust deposition can be differentiated into categories based on the amount of aeolian additions; soils developed from autochthonous materials with some aeolian additions, soils developed from autochthonous materials with aeolian additions as a major part, soils developed from aeolian materials on autochthonous rocks. The latter will be formed at deposition rates of about 10 g m^{-2} or more per year (Yaalon, 1987).

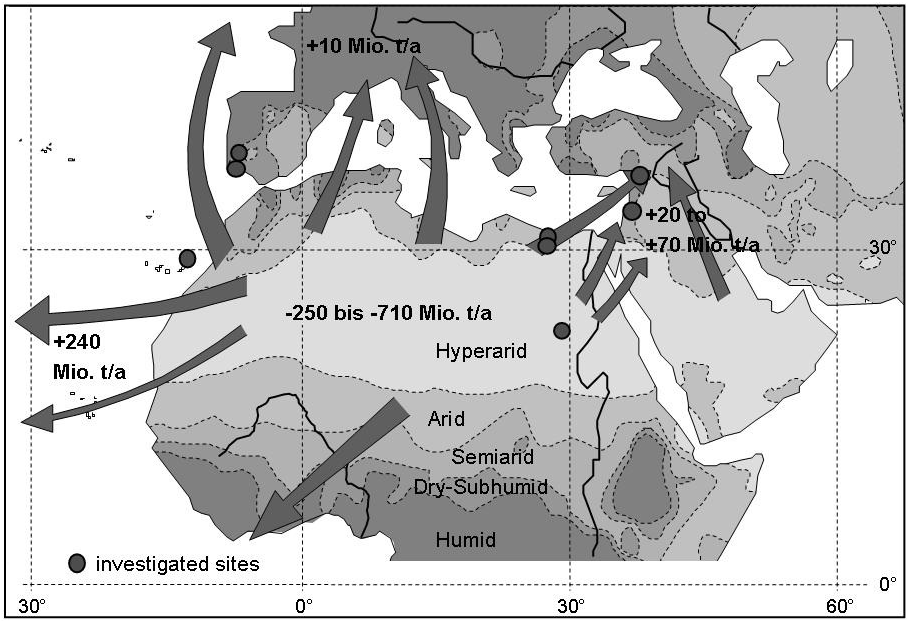

Figure 1. Transport trajectories of dust from the Saharan desert (according to Yaalon & Ganor, 1973; Péwé, 1982; Ganor & Mamane, 1982) and investigation sites.

Whereas pedogenesis is well described for soils derived from pure aeolian deposits (e.g. loess), information about the effects of aeolian additions on soil formation for soils developed mainly from autochthonous materials

containing only traces or minor parts of aeolian materials are still rare. Much progress has been made for the identification of aeolian additions. After more or less early qualitative descriptions, the analysis of oxygen isotopes in quartz grains (e.g. Jackson *et al*. 1971) and other mineralogical methods resulted in a broad knowledge about the fact of aeolian additions and possible source regions, but those studies seldom reflect the effect on pedogenesis.

Materials and Methods

Soils along a moisture gradient have been studied in Southern Egypt (on gneiss; P = <2 mm, T = 23°C), North West Egypt (on limestone, P = 40-130 mm, T = 20-21°C), Lanzarote/Canary Islands (on basaltic pyroclastics of different ages; P = 150-200 mm, T = 16-18°C), Israel (paleosols within basalt layers and recent soils on basaltic pyroclastics; P = 460-900 mm, T = 15-23°C), Southern Portugal (on limestone; P = 520-630 mm, T = 17-18°C) and Turkey (on serpentinite; P = 1090 mm, T = 15°C). A full description of the sites, soil data and methods used can be found in Jahn (1995).

Results

The investigated sites show very different signs of aeolian activity (Table 1). In all soils significant additions of aeolian material occur but decrease more or less along the moisture gradient. The site in the central part of the Saharan desert (S-Egypt) lost a huge amount of during the Pleistocene weathered material. The recent soil is mostly built up by locally redistributed material (developed from gneiss) and drifting sand of the adjacent occurring sandstone area. Drifting sand is also a significant contribution of the soils at the inner desert fringe in NW-Egypt. In all other soils the major aeolian contribution consists of far transported dust (almost silty).

Table 1. Investigated sites, autochthonous rock, time of soil formation and reconstructed aeolian additions.

Sites	Autochthonous rock	Estimated time of soil formation (ca. yr)	*Origin of soil mass in % of total soil mass (fine earth)*		
			Locally redistributed	*Local drifting sand*	*Far transported dust*
S-Egypt			huge loss by wind activity		
AH-2, -4, -7	Gneiss	?	65, 76, 66	20, 18, 25	- -
NW-Egypt					
P43, 24	Limestone	50,000	- -	30, 39	60, 41
Lanzarote					
IV_B-101, -303	Basaltic Pyroclastics	250	- -	?	4, 4
IV_A-605, -660	Basaltic Pyroclastics	6,000	- -	?	15, 22
III-502, -510	Basaltic Pyroclastics	40,000	- -	?	43, 25
III-570	Basalt	40,000	- -	?	66
Israel					
Shipon	Basaltic Pyroclastics	20,000	- -	?	2
1055	Basalt	30,000	- -	?	2
1052 (Paleosol)	Basalt	150,000	- -	?	17
Portugal					
Rod, Mol, Min, Gui, Bor	Limestone	200,000	- -	3, 9, 8, 5, ?	12, 16, 20, 13, 10
Turkey					
P161	Serpentinite	15,000	- -	1	2

Development of horizons

Aeolian activity in desert areas results in at least the development of two specific topsoil horizons (examples from Egypt). Many soils show due to wind erosion at the surface an enrichment of varnished and/or wind-shaped coarse rock fragments. Also the soil surface is mostly covered with a mm to some cm thick layer of well sorted aeolian sand. Below this sandy layer mostly a platy structured silty horizon with vesicular shaped coarse pores is developed (desert pan).

In the 250 year old Regosols from blackish basaltic pyroclastics of Lanzarote we could also observe a coarser grained upper layer and below the development of a brownish coloured horizon which contains mainly imported dust which was leached down from the surface. Quartz, kaolinite, illite and Fe-oxides of higher crystallinity qualify this fine material clearly as imported.

In well rubeficated limestone soils (examples from S-Portugal) with low organic matter content often a more brownish and silty A and B horizon can be observed in comparison to the soil material at the base of a profile or in between the rock fragments of a BC horizon.

Accumulation of organic matter
Dust samples often contain some percent of organic matter in the form of fragmented litter. Since very young soils in semiarid climates are not mature enough to support a plant cover (the Regosols in Lanzarote show only the growth of lichen at the surface layer), this imported organic matter is an important step for development of a pool of organic matter. To store this imported organic material it is important that the topsoil is coarse grained and the aeolian material can be washed down by the scarce rain events.
This imported organic matter may also increase the biological activity in the soil with the consequence of increasing the CO_2 content in the soil air and soil solution. This is an important prerequisite to enforce chemical weathering and to increase $CaCO_3$ solubility.

Carbonatisation
Dust samples contain, depending on the source region, carbonates (e.g. Lanzarote 18.5 %) and are on the one side a potential source for carbonatisation and on the other hand a buffer substance to inhibit weathering. The soils in S-Egypt contain 16-143 kg m^{-2} carbonates, far too much to explain the necessary Ca amounts by weathering e.g. plagioclases. Rough estimates make it probable to assume that about 20 % of Ca of the carbonates comes from plagioclases and therefore about 80 % should be imported.
In Lanzarote we could observe that only the dust samples and the younger soils contain carbonates in the form of pure $CaCO_3$ whereas in the older soils calcite is Mg substituted. This observation leads to the assumption that under the given climatical conditions only the first step of carbonatisation is initiated by the import of carbonates whereas in later stages (with increasing water holding capacity of soils) the dissolution of imported carbonates, weathering of the autochthonous parent material and (re)precipitation of carbonates occur. Therefore the very strong carbonatisation of the soils of the eastern Canary Islands should be based on two different sources of Ca. The data for the soils from more humid regions give no indications of carbonatisation processes or estimates of whether imported dust was carbonatic or not.

Texture development
Aeolian contributions may influence the texture development progressive as well as regressive from coarse to fine grained. In the coarse grained younger soils from pyroclastics the finer additions accelerate development of loamy texture classes (Figure 2). On the other side in more strongly developed soils from easy weatherable materials (basaltic pyroclastics, basalt, lime stone, serpentinite) the aeolian additions prevent at least the top soils becoming as clayey as the subsoils.

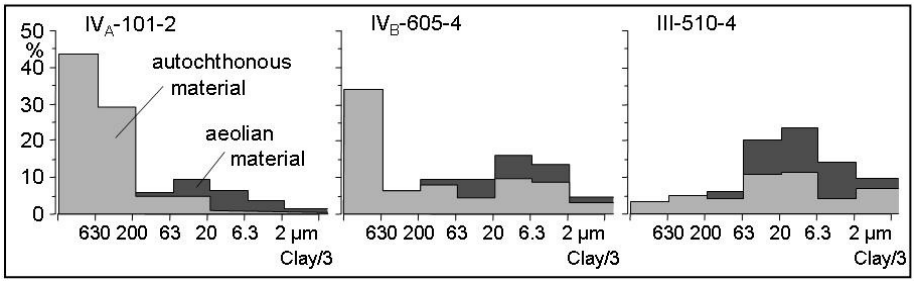

Figure 2. Reconstructed grain size distribution of autochthonous material (from pyroclastics) and of aeolian addition in different old horizons from Lanzarote.

Textures strongly influences the pore size distribution so the water and air regime of a soil will also be affected and in consequence most pedogenetic processes. Therefore in coarse grained soils aeolian additions increase water storage capacity, enables better plant growth in semiarid areas, increase litter fall and biological activity (see above) and also increase transformation processes for organic matter. In clayey soils the upper part is mostly more loamy developed under the influence of aeolian additions. Since aeolian additions are mostly dominated by non-swelling/-shrinking minerals, in the case of smectitic weathering of the autochthonous parent material (e.g. from basalt or serpentinite) the formation of peds is inhibited in the upper part. Often signs of stagnant conditions (Mn-coatings) can be observed in the transition zone of loamy and clayey horizons, even under semiarid to dry-subhumid conditions.

Development of mineral assemblage
Main constituents of aeolian sediments are quartz, illite and kaolinite. For soils developed from quartz-free autochthonous rocks, (beside other marker minerals) quartz is often used to quantify the influence of aeolian additions. Quartz grains occur in such cases usually as wind shaped grains of silt and fine sand size. In soils from rocks tending to form smectitic clay, from top to the bottom usually decreasing contents of illite and kaolinite can be found. Since the residuum of limestones is mostly also of a kaolinitic-illitic nature in such cases no diversification of clay assemblage is obvious.

Conclusion
Aeolian materials added to soils from an autochthonous rock may change soil forming processes in different ways. The size of impact is not only a function of the amount of added materials, it differs also according to the properties of the specific soil material from a certain rock and the stage of soil development. The impact on pedogenesis is generally stronger in younger soils than in older ones. The impact is also stronger in soils on rocks which are easy weatherable, like basaltic materials and sepentinite, than in soils on sedimentary rocks.

References
Ganor E, Mamane Y (1982) Transport of Saharan dust across the eastern Mediterranean. *Atmospheric Environment* **16**, 581-587.

Jackson ML, Levelt TWM, Syers JK, Rex RW, Clayton RN, Sherman GD & Uehara G (1971): Geomorphological relationship of tosposphericallyderived quartz in the soils of the Hawaiian Islands. *Soil Sci. Soc. Amer. Proc.* **35**, 515-525.

Jahn R (1995) Ausmaß äolischer Einträge in circumsaharischen Böden und ihre Auswirkungen auf Bodenentwicklung und Standortseigenschaften. Habilitationsschrift, *Hohenheimer Bodenkundliche Hefte* **23**. 213 p.

Lawrence CR, Neff JC (2009) The contemporary physical and chemical flux of aeolian dust: A synthesis of direct measurements of dust deposition. *Chemical Geology* **267**, 46-63.

Péwé TL (Edit.) (1981) Desert dust: Origin, characteristics and effect on man. *Geol. Soc. Amer. Spc. Pap.* **186**.

Yaalon DH, Ganor E (1973) The influence of dust on soils during the quaternary. *Soil Science* **116**, 146-155.

Loess, bioturbation, fire, and pedogenesis in a boreal forest – grassland mosaic, Yukon Territory, Canada

Paul T. Sanborn[A] and A.J. Timothy Jull[B]

[A]Ecosystem Science and Management Program, University of Northern British Columbia, Prince George, BC, Canada, Email sanborn@unbc.ca
[B]NSF-Arizona AMS Facility, University of Arizona, Tucson, AZ, USA, Email jull@u.arizona.edu

Abstract
Calcareous Holocene loess forms a surface veneer in soils of the topographically-controlled boreal forest – grassland mosaic near Kluane Lake, southwestern Yukon Territory, Canada. B horizons formed in Late Pleistocene / early Holocene loess have been buried by the continuing deposition of Neoglacial loess. These materials have been mixed in varying degrees with the underlying sandy glaciofluvial deposits by bioturbation and post-fire redistribution on slopes, creating a diversity of microstructures in the upper mineral and organic horizons. Contrasting soil types occur in close proximity under adjacent grassland and forest vegetation: Chernozemic (Kastanozem – WRB) and Brunisolic (Cambisol – WRB), respectively. The distribution of radiocarbon dates for soil charcoal preserved in toeslope colluvium suggests that fire activity diminished in the mid-Holocene.

Key Words
Loess, boreal forest, grasslands, fire, bioturbation, soil micromorphology

Introduction
Loess deposition has contributed to soil parent materials across the Beringian region of northwestern North America during the Quaternary (Muhs *et al.,* 2003; Sanborn *et al.,* 2006). Accessible opportunities to study soil formation in relation to contemporary loess deposition are available in relatively few areas in this region (Muhs *et al.,* 2004). This paper reports on the pathways of Holocene soil formation in relation to vegetation and natural disturbance processes in a complex boreal landscape in which loess deposition is currently active.

Study Area
The lower slopes of the Ruby Range on the southeastern shore of Kluane Lake (61º 3'N, 138º 21'W; Figure 1) are mantled by gravelly glaciofluvial deposits with up to 50 m of local relief and slopes up to 60%. Soils in the Kluane L region usually have a 10-30 cm thick veneer of calcareous loess, locally over-thickened to > 100 cm in depressions or on toeslopes. Loess accumulated in two phases: late Pleistocene / early Holocene and Neoglacial (Denton and Stuiver 1966). These deposits are often separated by a reddish-brown paleosol ("Slims soil") that forms the non-calcareous B horizon of many soils (Figure 2). Neoglacial loess can contain a 1-2 cm thick layer of the 1147 cal. yr BP White River tephra (Clague *et al.,* 1995). Rapid progradation of the Slims River delta after ca. 1700 AD (Clague *et al.,* 2006) created a closer dust source that likely accelerated loess deposition near Kluane L. The study area has a cold, dry climate, based on data for Haines Junction, 60 km southeast of the study area (mean air temperature -2.9ºC, mean annual precipitation 306 mm) (Environment Canada 2007). Slope aspect strongly influences microclimate and vegetation patterns. South- to west-facing aspects are usually occupied by *Festuca-Artemisia* grassland (Laxton *et al.,*1996), with abrupt transitions to boreal forest dominated by white spruce (*Picea glauca*), with lesser amounts of trembling aspen (*Populus tremuloides*) (Figure 3). The base-rich loessal grassland soils were designated as Melanic and Eutric Brunisols in the Canadian soil classification system (Laxton *et al.,* 1996; Soil Classification Working Group 1998), but those with organic matter-rich A horizons (Figure 4) are more appropriately placed in the Chernozemic order (Sanborn 2009), equivalent to Kastanozems (IUSS Working Group WRB 2006). Loessal soils on adjacent forested sites are predominantly Brunisolic (WRB – Cambisol), with Cryosols in some depressions and on north-facing toeslopes.

Methods
To examine soil property variation across vegetation boundaries, 31 pedons were described and sampled by pedogenic horizon (Soil Classification Working Group 1998) at 5- or 10-m intervals along three surveyed transects oriented perpendicular to the long axes of esker ridges, along slope segments with contours that were linear in plan view. Thin sections were prepared from epoxy-impregnated intact samples of selected horizons. Soil samples were analyzed for particle size distribution by pipetting (Gee and Bauder 1986), and for organic

and inorganic carbon before and after carbonate removal by HCl (LECO CHN-600 Elemental Analyzer). Charcoal was collected from toeslope colluvium at an additional 13 sites between Silver Creek and Cultus Bay (Figure 1), and was dated by accelerator mass spectrometry (Jull 2006), with radiocarbon ages converted to calendar years BP (cal. yr BP) using OxCal (Oxford Radiocarbon Accelerator Unit 2009) and the probability density function plotted.

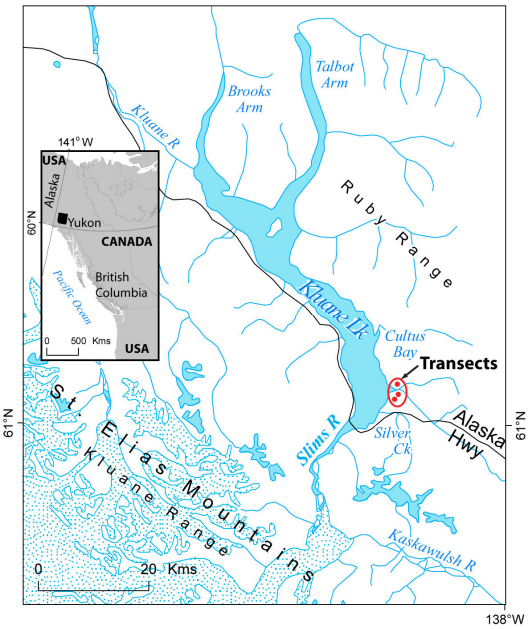

Figure 1. Study area location.

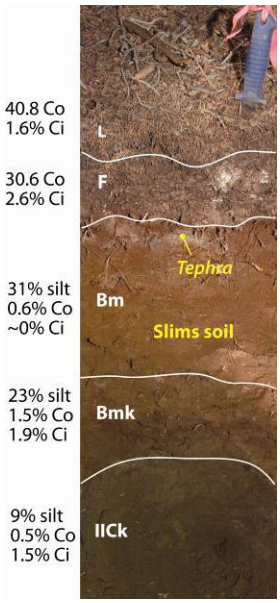

Figure 2. Brunisolic (WRB – Cambisol) forest soil, with high inorganic C (Ci) content in forest floor. (Co = organic C; knife handle = 11 cm long).

Results and Discussion

The three transects (45-82 m long, relief 12-20 m) were located ~9-11 km from the Slims River delta (Figure 1). Grass-dominated vegetation occupied the upper 2/3 of slopes with aspects ranging from 230° to 260°, while boreal forest occupied all other slope positions. Controlling for slope steepness, pedons on upper- and midslope positions did not differ significantly between forest and grassland in the thickness-weighted silt content of the uppermost 50 cm of mineral soil (t-test: p=0.42, df=6). Although forest should intercept and retain dust more efficiently than low herbaceous vegetation (Muhs *et al.,* 2003), our sample size may have been too small to detect such an effect. This comparison also did not attempt to estimate the amounts of aeolian material retained in forest floors.

For a majority of transect pedons, some degree of mixing of parent materials has occurred, as indicated by coarse fragments and/or sandy loam textures in the uppermost mineral horizons (e.g. Figures 2,3). The White River tephra, associated with the Neoglacial loess, was present as a recognizable marker layer (e.g. Figure 2) in only 50% of the transect pedons, and displayed > 50 cm of lateral continuity in only one case. Bioturbation was likely responsible for this morphological disruption and variability, with different agents predominating under different vegetation types: arctic ground squirrels (*Spermophilus parryii*) in grasslands (Zazula *et al.,* 2006) (Figure 5), and tree-throw in forests. The extent of bioturbation influenced microstructure formation (Figures 6a,b), with silt-rich B horizons displaying platiness created by seasonal ice lens formation (Van Vliet-Lanöe 1985), while there was little or no aggregation in A and B horizons with coarser textures that resulted from mixing of loess with underlying glaciofluvial sands and gravels.

The fate of Neoglacial loess in surface horizons differed between forest and grassland soils. Forest floors resembled mor humus (Figure 2), but with L and F horizons that were visibly enriched in silt (Figures 6c,d) and detrital $CaCO_3$ (mean inorganic C concentrations: L – 2.2%, n=11; F – 1.4%, n=13). Grassland soils lack surface organic horizons, but loess inputs appeared to be initially incorporated in biological soil crusts (Figure 4) (Marsh *et al.,* 2006), except in areas disrupted by recent squirrel burrowing (Figure 5).
Reworking of loess on forested slopes during the Holocene may have also occurred after fires, based on the association between charcoal and buried soils in toeslope colluvium. The exact mechanism of post-fire redistribution is uncertain, given the dry climate that would make water erosion unlikely. The cumulative

probabilities of the calibrated radiocarbon dates for soil charcoal suggested a mid-Holocene decline in fire activity (Figure 7). This was consistent with the record of charcoal accumulation rates in a small pond within 5 km of the sites examined in this study (Whittmire 2001). However, the absence of soil charcoal dates between ~ 3000 and 6000 cal. yr BP could also reflect reduced loess deposition during a period of diminished glacial sediment production, and hence, less potential for burial and preservation of soil charcoal by colluviated loess.

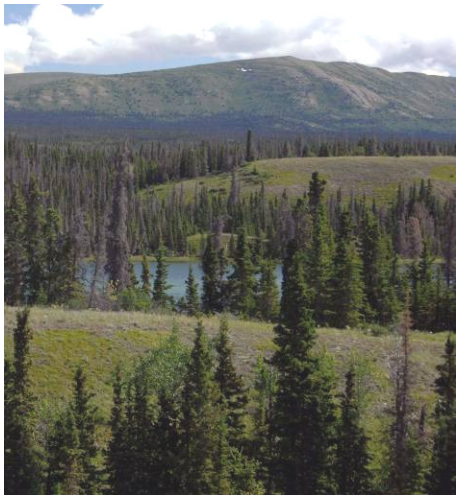

Figure 3. Intermingled grassland and boreal forest vegetation on esker ridges, between Ruby Range and Kluane L. Grassland in foreground has slope aspect of 260º.

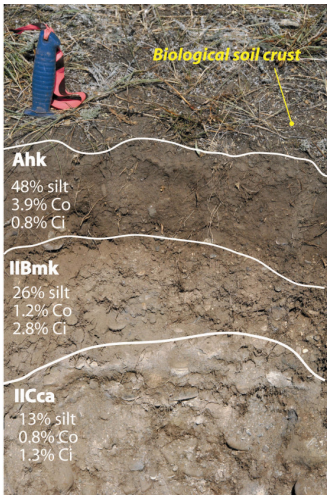

Figure 4. Chernozemic (WRB – Kastanozem) soil on crest of esker ridge. (Co = organic C; Ci = inorganic C; knife handle = 11 cm long)

Figure 5. Recent soil disturbance by arctic ground squirrels (*Spermophilus parryii*) in grassland.

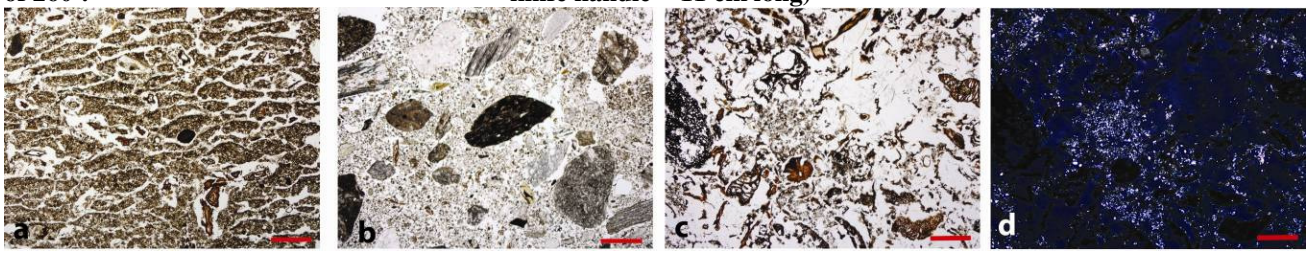

Figure 6. Thin section views (plane light, except as noted): (a) platy structure in silt-rich B horizon of forest soil (depth ~ 20 cm), (b) weakly aggregated B horizon of grassland soil, (c) forest organic surface horizon with high silt content, (d) same view as (c), but with crossed polarizers. Scale bar = 1 mm.

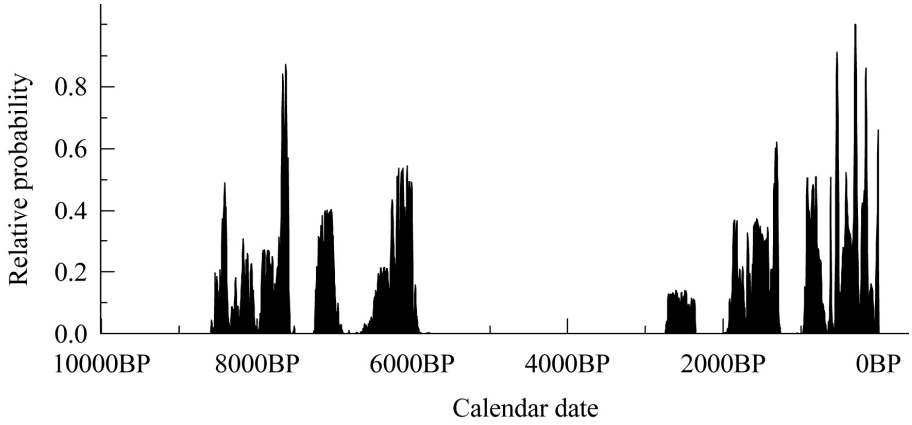

Figure 7. Cumulative probabilities of calibrated accelerator radiocarbon dates for soil charcoal (n=23).

Conclusions

Pedogenic modification of Holocene loess has followed diverging pathways in topographically-controlled forest-grassland mosaics in southwestern Yukon. Calcareous surface horizons of grassland soils displayed varying degrees of mixing of loess with the underlying glaciofluvial sands and gravels. Arctic ground squirrels (*Spermophilus parryii*) have been a major agent of soil bioturbation in these grasslands. In contrast, forest soils had mor-like surface organic horizons that were visibly enriched in calcareous silt. Redistribution of loess on forested slopes likely occurred through a combination of bioturbation by treethrow and episodic soil movement after fire. Variable mixing of these parent materials has created a diversity of microstructures in upper mineral horizons. Radiocarbon dating of soil charcoal preserved in toeslope colluvium suggests that fire activity diminished in the mid-Holocene.

Acknowledgements

We thank Ekaterina Daviel for field assistance. Dan Pennock (Univ. Sask.), Mary Vetter (Univ. Regina), Brad Hawkes (Can. Forest Serv.) and Scott Smith (Agric. Agrifood Can.) provided helpful advice. Funding was provided by the Natural Sciences and Engineering Research Council and the National Science Foundation.

References

Clague JJ, Evans SG, Rampton VN, Woodsworth GJ (1995) Improved age estimates for the White River and Bridge River tephras, western Canada. *Canadian Journal of Earth Sciences* **32**, 1172–1179.

Clague JJ *et al.* (2006) Rapid changes in the level of Kluane Lake in Yukon Territory over the last millennium. *Quaternary Research* **66**, 342-355.

Denton GH, Stuiver M (1966) Neoglacial chronology, northeastern St. Elias Mountains, Canada. *American Journal of Science* **264**, 577-599.

Environment Canada (2007) Canadian Daily Climate Data. CD-ROM.

Gee GW, Bauder JW (1986) Particle-size analysis. In 'Methods of Soil Analysis. Part I. Physical and Mineralogical Methods'. (Ed A Klute), pp. 331-362. (Soil Science Society of America: Madison).

IUSS Working Group WRB (2006) World Reference Base for Soil Resources 2006. World Soil Resources Reports No. 103. (FAO: Rome).

Jull AJT (2006) Radiocarbon dating: AMS method. In 'Encyclopedia of Quaternary Science'. (Ed. S Elias), pp. 2911-2918. (Elsevier: Amsterdam).

Laxton NF, Burn CR, Smith CAS (1996) Productivity of loessal grasslands in the Kluane Lake region, Yukon Territory, and the Beringian "Production Paradox". *Arctic* **49**, 129-140.

Marsh J, Nouvet S, Sanborn P, Coxson D. 2006. Composition and function of biological soil crust communities along topographic gradients in grasslands of central interior British Columbia (Chilcotin) and southwestern Yukon (Kluane). *Canadian Journal of Botany* **84**, 717-736.

Muhs DR *et al.* (2003) Stratigraphy and palaeoclimatic significance of Late Quaternary loess-paleosol sequences of the Last Interglacial-Glacial cycle in central Alaska. *Quaternary Science Reviews* **22**, 1947-1986.

Muhs DR, McGeehin JP, Beann J, Fisher E (2004) Holocene loess deposition and soil formation as competing processes, Matanuska Valley, southern Alaska. *Quaternary Research* **61**, 265-276.

Oxford Radiocarbon Accelerator Unit (2009) OxCal (v. 4.1) http://c14.arch.ox.ac.uk/oxcal.html

Sanborn PT (2010) Topographically-controlled grassland soils in the Boreal Cordilleran ecozone, northwestern Canada. *Canadian Journal of Soil Science* **90**, 89-101.

Sanborn PT, Smith CAS, Froese DF, Zazula GD, Westgate JA (2006) Full-glacial paleosols in perennially frozen loess sequences, Klondike goldfields, Yukon Territory, Canada. *Quaternary Research* **66**, 147-157.

Soil Classification Working Group (1998) The Canadian System of Soil Classification (3rd ed.). Publication 1646 (Agriculture and Agri-Food Canada, Ottawa).

Van Vliet-Lanöe B (1985) Frost effects in soils. In'Soils and Quaternary Landscape Evolution'. (Ed. J Boardman), pp. 117-158 (Wiley, New York).

Whittmire CM (2001) Vegetation and fire history of the area surrounding Keyhole Pond, Yukon Territory. M.Sc. Thesis. (Univ. Regina: Regina).

Zazula GD, Mathewes RW, Harestad AS (2006) Cache selection by arctic ground squirrels inhabiting boreal-steppe meadows of southwest Yukon Territory, Canada. *Arctic, Antarctic, and Alpine Research* **38**, 631-638.

Micromorphology of a welded paleosol in the Dillondale loess, Charwell Basin, South Island, New Zealand

Carol Smith[A], Matthew Hughes[A], Peter Almond[A] and Philip Tonkin[A]

[A]Department of Soil and Physical Sciences, Faculty of Agricultural and life Sciences, PO Box 84, Lincoln University, New Zealand.

Abstract
Micromorphological evidence and soil phosphorus chemical data supporting the presence of a welded paleosol from the Dillondale loess are presented. Since both topdown and upbuilding pedogenesis can occur in loess deposits, welding of paleosols will occur when topdown pedogenesis overprints an existing paleosol. Intact soil samples were collected and their micromorphology described, and soil P fractions were determined. The micromorphology and soil P fractions provide strong evidence for a welded soil between 3.0 and 4.0 m depth (L3b basal unit). Throughout this unit the b-fabric is both porostriated and granostriated; amorphous concentration features are moderately to strongly impregnated, postdating clay cutans. We interpret this to reflect greater mechanical stress on the clay domains and hence a longer period of topdown pedogenesis. Low levels of P_{Ca} and a high proportion of P_{Occ} in the L3b basal unit imply these are highly weathered horizons. This suggests two phases of topdown pedogenesis during a hiatus in loess accretion. We propose that an extended period of illuvial clay deposition in the underlying b2Btg1 and b2Btg2 horizons occurred, reducing macropore continuity in the horizons above. Intense anaerobic conditions would have resulted, with the onset of gleying and the formation of the amorphous concentration pedofeatures.

Key Words
Micromorphology, welded paleosol, loess, pedogenesis, pedofeatures

Introduction
Fragmentary terrestrial records such as loess deposits constitute important archives of Quaternary environmental change. In New Zealand, loess is an extensive deposit commonly occurring on Pleistocene and Holocene river terraces. Loess-paleosol stratigraphic studies supported by luminescence and radiocarbon dating and tephrochronology suggest that the majority of loess deposits are less than 300 ka old (Schmidt *et al.* 2005). Pedogenic alteration within the loess deposits is driven by temporal variation of both the rate of loess accretion and external climatic factors. Pedogenesis within the loess accretionary column occurs in two phases: during active accretion, known as upbuilding (weak pedogenesis); and during hiatuses in loess accretion, known as topdown (strong pedogenesis in warmer and wetter periods when no new sediment accumulates) (Almond and Tonkin 1999; Lowe *et al.* 2008). Ruhe and Olson (1980) defined welded soils as those formed when pedogenesis from an overlying soil extends down into and overprints a lower soil. Loess accretionary columns can contain paleosols comprised of both accretionary and welded components – named pedocomplexes by Kemp *et al.* (1994). Welded soils can thus obscure details of the loess stratigraphy and hence events associated with Quaternary climatic change can be missed. To tease apart the phases of pedogenesis obscured in the morphology, chemical and micromorphological analysis can be used. In this paper we focus on the micromorphology of a striking buried paleosol in the third (basal) loess sheet of a 3-loess sheet sequence found in north-eastern South Island, New Zealand. The paleosol is thick, very clay rich, when compared to surface soils, and shows spectacular reductimorphic features including large Mn nodules and a network of horizontal and vertical gley veins. Our results refine the present loess stratigraphy and contribute to a better understanding of paleoenvironment in this part of NZ in the Late Quaternary.

Methods
Samples were taken from a loess section exposed in a cliff face cut in the Dillondale terrace. The buried soil developed in L3 was sampled at 287 mm (b2Bt(g)); 330 mm (b2Btgc1) and at 399 mm (b2Btg2). Samples were also taken from the L1 and L2 sheets higher up in the section for comparison (sampled at 138 mm, 169 mm (Bx(g); 189 mm (bBw(g)), 205 mm (bBcg) and 240 mm (bBt(g)). Soil blocks were prepared according to standard procedures (Lee and Kemp, 1992) and thin sections were described according to Bullock *et al.* (1985). Fabric features described included b-fabric, excremental infillings, clay lamellae, laminated and non-laminated cutans, fragmented cutans and amorphous crystalline segregations. Phosphorus fractions for the Dillondale interfluve section were determined at each 10 cm interval for the first 1 m, and then at every 20 cm for the remainder of the loess column. Detailed methods are reported in Hughes *et al.* (in prep). Total soil P (P_T) was

1 – 6 August 2010, Brisbane, Australia. Published on DVD.

determined using the sodium hydroxide fusion method of Smith and Bain (1982) while organic phosphorus (P_{Org}) was determined using a method adapted from Bowman (1989) Total inorganic P (acid+base) subtracted from estimated total P (acid+base) gives P_{Org}. Organic P (P_{Org}) subtracted from P_T determined by the Smith and Bain (1982) method gave inorganic P. The non-occluded phosphorus fractions of this (P_{Ca} and $P_{Fe/Al}$) were determined using an acid and base extraction method adapted from Murphy and Riley (1962). All P fraction extracts were analysed on a Varian Cary 50 ultraviolet/visible spectrophotometer set at 880 nm wavelength. The occluded fraction was calculated as the difference between total inorganic P and P_{Ca}+$P_{Fe/Al}$. (Hughes *et al.* in prep).

Results and Discussion

Phosphorus fractions

Total P: From the top of L3 downwards, there was a slight increase in P_T before subsequent decreases in the b2Btgc1 and b2Btgc1 horizons. Total P peaked at the top of the b2Btg horizon at ~3.8 m, before decreasing to 221 µg/g at 4.1 m, then increased to 292 µg/g at the base of L3 (Figure 1.). P fractions: P_{Occ} dominated, peaking at 70% of P_T at 3.7 m, while $P_{Fe/Al}$ comprised the second dominant fraction peaking at 55% at 3.1 m. These two peaks in absolute concentrations coincided with two distinct peaks in relative abundance of P_{Org}. Apatite P (P_{Ca}) comprised a relatively low percentage of P_T in the upper half of L3, but increased to 19% at the base of L3. P_{Ca} makes up a significant component of the least weathered, lower subsoil peaks in each loess sheet. P_{Occ} reaches maxima in horizons persisting at the surface for long periods and in deep subsoils (e.g. Bwg, Bxg), and minima in gleyed upper subsoil horizons (e.g. Btg, Bcg). P_T and P_{Ca} are lower in L2 and L3 suggesting they are more weathered than L1, and the very low P_{Ca} and high proportion of P_{Occ} in the upper part of L3 suggests these are the most weathered horizons of all. Organic P makes up a high proportion of P_T in the A horizon of the surface soil, but persists as in the upper parts of buried soils as well. Organic P showed a broad peak centred at the L2/L3 boundary that overlapped with relatively high levels in the base of L2. A secondary peak occurred at 3.5 m in the b2Btgc2 horizon (Figure 1).

Micromorphology

The micromorphology of the L3a (b2Bt(g)) is noticeably different when compared to the L3b unit. The b-fabric in the L3a is granostriated only, and there are few amorphous concentration pedofeatures. In the b2Bt(g) horizon, excremental fabric is readily apparent, postdating the amorphous concentration pedofeatures therein. Cutans are extensive and postdate or are contemporaneous with the excremental fabric. We interpret this to reflect one period of topdown pedogenesis only, since there are fewer amorphous concentration pedofeatures and the b-fabric is granostriated, suggesting that less intense physical stresses were involved in realigning the clay domains.

Towards the base of the L3b (b2Btg2) there is a prominent macro vein and prism structure, but excremental fabric is absent. The veins contain clay and silt cutans while the b-fabric therein is both porostriated and granostriated. The prisms contain some redox segregations adjacent to the prism faces. At the top of the L3b (b2Btgc1), the b-fabric is also porostriated and granostriated. In the b2Btgc1, there are noticeably more amorphous concentration pedofeatures compared to the b2Btg1 below, and these postdate the majority of clay cutans. We propose that an extended period of illuvial clay deposition in the underlying b2Bt1 and b2Btg2 horizons occurred – reducing macropore continuity in the overlying b2Btgc1 and b2Btgc2 horizons. Intense anaerobic conditions would have resulted in these horizons, (more so in the b2Btgc1) with the onset of gleying and the formation of the amorphous concentration pedofeatures.

Porostriated b-fabric is indicative of considerable shrink/swell activity; the stress induced by alternating cycles of wetting and drying causing the realignment of clay domains. This fabric is to be expected in the veins of the b2Btg2 horizon, due to the considerable shrink-swell processes associated with vein and prism morphology. We infer this to reflect an intense and long-lived phase of pedogenesis. We propose that the welded soil in b2Btgc1 resulted from two separate phases of intense pedogenesis; phase one (long and intense) and phase two (shorter, and less intense), separated by a loess accretion phase. Micromorphological evidence for a welded horizon in this situation would include the overprinting of the existing subsurface morphology in b2Btgc1 with further subsurface features. If the overlying loess sheet is thin enough, the second phase of pedogenesis would drive both the morphology of the L3a (b2Bt(g)) and the underlying L3b (b2Btgc1).

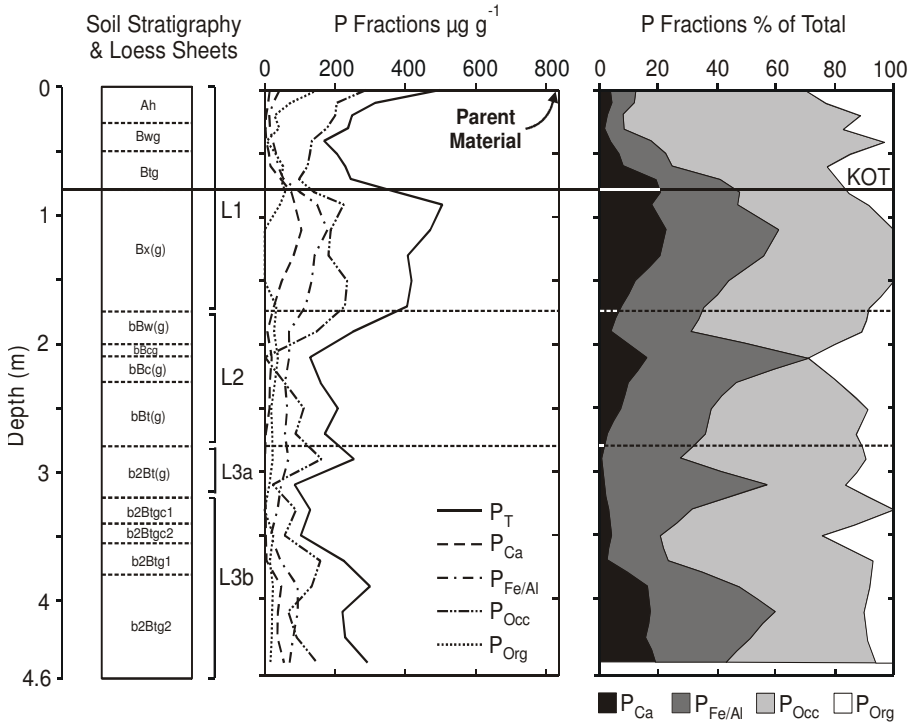

Figure 1. Phosphorus fractions presented as absolute values (centre) and percentages of total values (right). Soil stratigraphy and loess sheet delineations are presented on the left. P_T = total P, P_{Ca} = apatite P, $P_{Fe/Al}$ = Fe- and Al-bound P, P_{Occ} = occluded P, P_{Org} = occluded P. Also shown is the value (P_T) of river silt parent material, and the stratigraphic location of the ca. 27 ka Kawakawa/Oruanui Tephra (KOT; solid line). Figure reproduced from Hughes *et al.* (2010) (in prep.).

Thus subsurface processes will overprint on existing subsoil morphology. We infer overprinting from the intensity of the micromorphological features developed therein, in the top of the L3b (b2Btgc1): porostriated b-fabric and the moderately-strongly impregnated amorphous concentration features postdating the majority of clay cutans. This overprinting is supported by the phosphorus chemical data: (very low P_{Ca} and high proportion of P_{Occ} in the upper part of L3) implying a highly weathered horizon.

Conclusion

Both the micromorphology and the soil P chemistry strongly suggest that a welded soil can be distinguished in the L3b, between 3.0 and 4.0 m depth. We conclude that welding occurred as a result of two phases of topdown pedogenesis, punctuated by a short period of loess accumulation of ~0.5 m and associated pedogenic upbuilding. This would have resulted in two separate periods of clay illuviation and associated gleying conditions. Topdown pedogenesis in L3a affected both the more recently aggraded loess and also the top of the underlying L3b unit (b2Btgc1 horizon).

References

Almond PC, Tonkin PJ (1999) Pedogenesis by upbuilding in an extreme leaching and weathering environment, and slow loess accretion, south Westland, New Zealand. *Geoderma* **92**, 1-36.

Bowman RA (1989) A sequential extraction procedure with concentrated sulfuric acid and dilute base for soil organic phosphorus. *Soil Science Society of America Journal* **53**, 362-366.

Bullock P, Fedoroff N, Jongerius A, Stoops G, Tursina T (1985) 'Handbook for Soil Thin Section Description'. (Waine Research Publications: Wolverhamption).

Fedoroff N, Courty MA, Thompson ML (1990) Micromorphological evidence of paleoenvironmental change in Pleistocene and Holocene paleosols. In 'Soil Micromorphology: a basic and applied science'. (Ed LA Douglas) pp. 653-665. (Elsevier: Amsterdam).

Hughes MW, Almond PC, Smith CMS, Tonkin PJ (in prep). Econstructing late Quaternary environmental change in Charwell Basin, South Island, New Zealand – Part I: Loess stratigraphy, pedogenesis and chronology. *Quaternary International*

Kemp RA, Jerz H, Grottenthaler W, Preece RC (1994) Pedosedimentary fabrics of soils within loess and colluvium in southern England and Germany. In 'Soil Micromorphology' (Ed A Ringrose-Voase G Humphries) pp. 207-219. (Elsevier: Amsterdam).

Lee J, Kemp R (1992) 'Thin sections of unconsolidated sediments and soils: a recipe'. CEAM Technical Report no. 2. Centre for Environmental analysis and Management. Royal Holloway, University of London.

Lowe DJ, Tonkin PJ, Palmer AS, Palmer JA (2008) Dusty Horizons. In 'A Continent on the Move' New Zealand Geoscience Into the 21st Century. (Ed I Graham I). pp 270-273. (GSNZ Miscellaneous Publication 124).

Ruhe RV, Olson CG (1980) Soil welding. *Soil Science* **130**, 132-139.

Schmidt J, Almond PC, Basher L, Carrick S, Hewitt AE, Lynn IH, Webb TH (2005) Modelling loess landscapes for the South Island, New Zealand, based on expert knowledge. *New Zealand Journal of Geology and Geophysics* **48**, 117-133.

Smith BFL, Bain DC (1982) A sodium hydroxide fusion method for the determination of total phosphate in soils. *Communications in Soil Science and Plant Analysis* **13**, 185-190.

Quantifying the soil- and ecosystem-rejuvenating effects of loess in a high leaching environment, West Coast, New Zealand

Andre Eger, Peter C. Almond and Leo M. Condron

Faculty of Agriculture and Life Sciences, Lincoln University, P.O. Box 84, Canterbury, New Zealand, Email andre.eger@lincolnuni.ac.nz

Abstract
Ecosystem succession through pioneer, seral, climax and finally retrogressive communities is usually strongly associated with biogeochemical accession of soil nutrients. In leaching-driven, humid environments, retrogression is known to coincide with soil nutrient decline, particularly soil P. Counteracting this tendency are rejuvenating processes, included within what has been referred to as regressive pedogenesis, which replenish soil nutrients. Despite large areas of old landsurfaces, ecosystem retrogression seems to be rare, indicating that rejuvenation processes are effective in avoiding ecosystem decline. Regressive pedogenesis, however, has received little attention despite its importance for ecosystem evolution.
In this paper we quantify the regressive effect of loess on soil and ecosystem properties in a superhumid, high leaching environment on the west coast of the South Island, New Zealand. A dune sequence downwind of a riverbed loess source provides a gradient of loess flux, and away from loess deposition, an age gradient (chronosequence). Coincidence of property values between the soils of the loess gradient on the oldest (6500 y old) dune and the chronosequence allow an 'apparent soil age' for a given loess flux to be estimated. A regression index calculated from dune age and apparent age quantifies the regressive effect of the loess flux. Early results show the regressive effect of loess is retarding podsol formation and increases foliar nutrient content. This effect seems to reach no further than to 1000 m from the source of the loess. Soil pH does not show any relation to loess accretion. Further work is currently underway to determine more soil and ecosystem properties in order to quantify the regressive effect of loess on these properties. These results will be available at the time of the conference.

Key Words
Regressive pedogenesis, atmospheric deposition, loess, ecosystem retrogression, soil chronosequence

Introduction

Soil chronosequence studies under unmodified vegetation have demonstrated a co-evolution of soils and ecosystems. In humid environments where leaching drives ongoing nutrient loss, some soil chronosequence studies show that after initial successional phases with increasing biomass, diversity and soil fertility, ecosystems can go into a state of decline (Chadwick *et al.* 1999; Wardle *et al.* 2008). This retrogressive phase has been shown to occur once thresholds of nutrient availability, particularly soil P, are crossed (Richardson *et al.* 2004; Walker and Syers 1976). Despite the large area of humid zones on Earth, including land surfaces of great antiquity, ecosystems in a state of retrogression are rare, suggesting that processes of soil rejuvenation are effective at replenishing nutrients. This tendency for rejuvenation of the soil system is captured in Johnson and Watson-Stegner's (1987) soil evolution model. A progressive vector, which is viewed as resulting in soil deepening, horizonation and chemical depletion, is counteracted by a regressive vector which includes soil mixing, shallowing or incorporation of new mineral material that homogenises the soil or increases its chemical reactivity and fertility. Johnson and Hole (1994) argue that while there has been a lot of research driven by a focus on the soil forming factor model of soil development, there has been little attention on regressive processes, which is equally true for ecosystem decline (Wardle *et al.* 2004). Yet, these processes are clearly important for understanding trajectories of soil and ecosystem evolution.
On the superhumid west coast of the South Island of New Zealand, soil chronosequence studies on sequences of glacial moraines have documented a moss/lichen-shrub-angiosperm/conifer forest succession culminating in ecosystem retrogression on landsurfaces > 100,000 y old. The retrogressive phase is characterised by shrub, stunted conifers and heath vegetation (Richardson *et al.* 2004; Wardle *et al.* 2004). The parallel soil evolution is from Entisols to Inceptisols to Spodosols (Sowden 1986; Stevens 1968). As elsewhere, despite the presence of significant areas of landsurfaces > 100,000 y old (GNS Science 2008), ecosystems in a state of retrogression are relatively rare. In this paper we examine the role of loess as a vector of regressive pedogenesis and a mitigator of ecosystem nutrient depletion in this superhumid environment. We develop a new conceptual framework and an index to quantify the regressive effects of loess.

1 – 6 August 2010, Brisbane, Australia. Published on DVD.

Study area

The study area is a sequence of shore-parallel coastal dunes on the prograding coastal plain west of the Southern Alps, north of the mouth of Haast River, South Island, New Zealand (MAT 11.3°C, precipitation 3455 mm/a; Hessel 1982). The dune ridges are densely forested with unmodified temperate rainforest consisting of conifers (*Dacrydium cupressinum*, *Prumnopitys ferruginea*) and angiosperms (*Weinmannia racemosa*, *Metrosideros umbellata*).

The oldest dune is ca 6500 years old, forming soon after the culmination of the post-glacial sea level rise (Gibb 1986). Younger dunes represent phases of coastal progradation and dune building associated with pulses of sediment brought down the Haast River. At least for the youngest six dunes, these sediment pulses correspond to periods immediately after large earthquakes generated on the range-bounding Alpine Fault (Wells and Goff 2006). The dune ridges have relief which varies from ca 2 to 15 m and are generally continuous or semi-continuous for up to 8 km. A uniform quartzo-feldspathic sand parent material, low variation in the Holocene climate and an undisturbed native vegetation cover (Eger and Almond in prep.) offer good conditions for soil and ecosystem chronosequence studies (Dickinson and Mark 1994; Palmer *et al.* 1986). A previously unpublished report by Palmer *et al.* (1986) presents four soil profiles of 360, 1000, 3000 and 6500 years of age. The sequence progresses from a typic udipsamment (acid brown soil) to several stages of placorthods (podsols). Throughout the Holocene the braided Haast River has extended seaward and its bed has provided a source of silt which has been deflated by the dominant south-westerly winds (Marx and McGowan 2005), and now drapes the dunes. The loess mantle is limited to within 2 km down-wind of the river. The dune sequence thus provides two soil gradients: first, a gradient of soil age from youngest to oldest dune which we assume is only minimally affected by the regressive effect of loess, and second, a gradient of loess accession which decreases from close to the river to distant from the river (Figure 1).

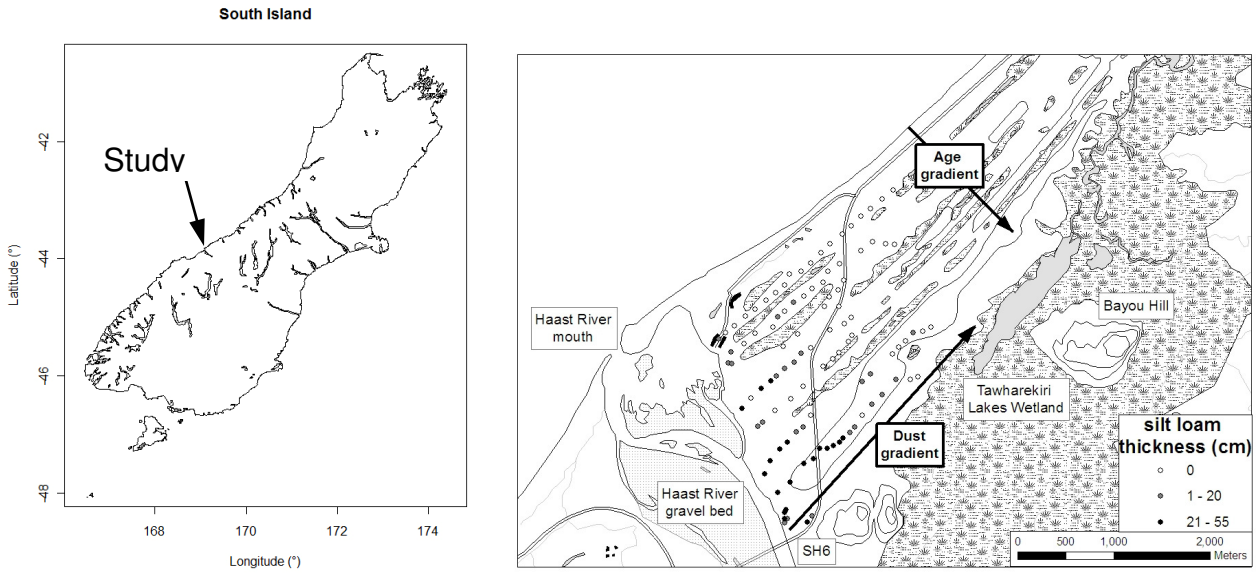

Figure 1. Location of the study area, the dune sequence NE of Haast River, with age and loess gradient.

Conceptual Framework and Methods

Our approach to quantifying regressive pedogenesis is based on the principle that addition of loess, if regressive, will result in a soil of a given age having properties consistent with those of a younger soil. How much younger quantifies the strength of the regressive effect. We calibrate the regressive effects of the loess by comparing soil chemistry and vegetation nutrient status along the loess gradient with chronofunctions of the same properties derived from the chronosequence. This concept is shown in Figure 2 where the red line shows a hypothetical chronofunction, and the blue line represents variation of the same soil or ecosystem property along the gradient of loess accumulation on the oldest (6500 y old) dune. A Regression Index (RI) is calculated from the ratio of apparent age of the soil ($S_{(age)}$), as adjudged by comparing soil/ecosystem properties with those of the chronosequence, to the age of the underlying dune ($P_{(age)}$ = 6500 y), as

RI = 1 - $S_{(age)}/P_{(age)}$. Where there is no loess flux we expect $S_{(age)} \approx P_{(age)}$, and therefore RI ≈ 0; where the loess flux has had some regressive effect, $S_{(age)} < P_{(age)}$ and therefore RI > 0.

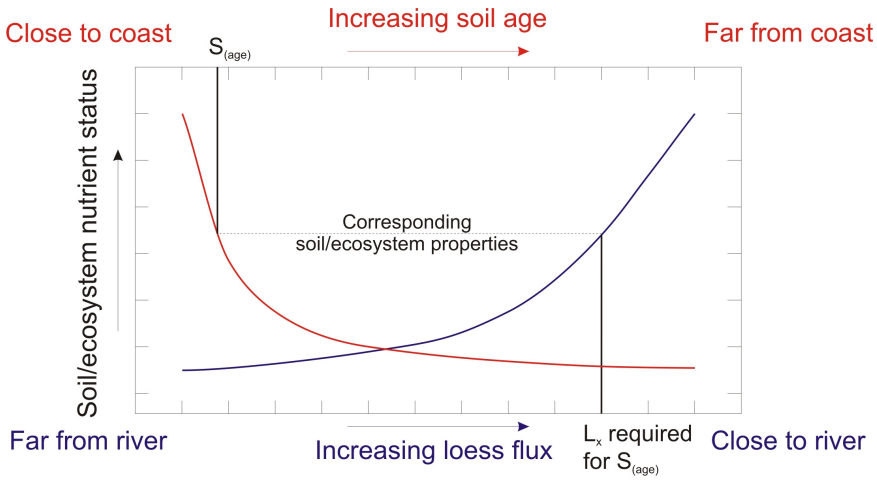

Figure 2. A hypothetical chronofunction for a soil/ecosystem property (red) and variation of the same property along the loess flux gradient on the 6500 y dune (blue). The apparent age $S_{(age)}$ of the soil affected by loess flux L_x is equal to the age at which a soil on the chronosequence would have the same value of that property.

Spatial variability of the loess flux was determined by an auger survey of the dune ridges, comprising ~100 sites drilled at 100-150 m intervals to a depth of 50 cm. So far, seven soil pits have been dug along the oldest dune to a depth of at least 130 cm, and sampled by corer according to soil horizons in 7.5 cm increments or less in the upper 50 cm, and 15 cm increments below 50 cm depth. Soil samples were dried, sieved to < 2 mm and analysed for pH (Blakemore *et al.* 1987), total element content by XRF (van Reeuwijk 2002), oxalate, pyrophosphate and dithionite extractable Al and Fe (Blakemore *et al.* 1987), different P fractions (Chen *et al.* 2000) and carbon/nitrogen by dry combustion (Burt 2004). Particle size distribution was determined according to the pipette method, after removal of organic matter and iron oxides from samples (Burt 2004), bulk density was determined from core samples and the compliant cavity method (Burt 2004).
A reconnaissance sampling of tree foliage from *Prumnopitys ferruginea*, *Dacrydium cupressinum* and *Weinmannia racemosa* was done at each soil pit site, using a shotgun to collect fully expanded, fresh leaves of sunlit branches. The leaves were stored in the dark and kept cool until processing in the laboratory. Sampling time was late February to early March when leaves are fully developed. Samples were dried, ground and digested in HNO_3 and analysed by ICP (Richardson *et al.* 2004).

Preliminary results

Along the chronosequence, increased horizonation is illustrated both morphologically and chemically by development of eluvial (E) and illuvial horizons (Bfm, Bh, Bs) over 1000 years of pedogenesis. Losses of soil nutrients are especially strong during the first 1000 years. At the oldest site, the amounts of P, Ca, K and Na are severely depleted to only 25%, 48%, 38% and 46% of the original parent material values, respectively. Initial profile dilation (+58%) mostly as a result of organic matter accumulation after 360 years becomes collapse (-36%) at the oldest site. The spatial variation of loess flux is reflected in the variation of thickness of a surface silt loam mantle over dune sand, which is thickest on the oldest dune and thins with increasing distance from the river bed (Figure 1). Reflecting their age, the younger dunes have received much less eolian material confined to locations very close to the river bed. Along the loess gradient, the decrease of the soil silt content (kg/m² for the upper 50 cm) in six selected soils on the oldest dune is statistically significant (e.g. for a log model: silt = a * log(distance) + z; $R^2 = 0.90$, $p < 0.01$).
The loess flux has a regressive effect on soil morphology. Closest to the river where silt loam thickness is 34 cm, the soil has the most weakly expressed podsol features, and loess accretion appears to be contributing to formation of an upbuilding Bw horizon (Almond and Tonkin 1999). Further away from the river, typical podsol characteristics become increasingly distinct. Well expressed eluvial/illuvial horizons and broken iron pans develop from 500 m away from the river under a thinner silt loam mantle of between 18 and 27 cm thickness. At a distance of >1800 m, silt loam textures are absent and the soils show continuous cemented iron pans. In contrast, there is no apparent regressive effect of the loess flux with respect to soil pH. The depth relationship is very similar in all studied profiles with very low values (<4) in the H horizons, values between 4 and 5 in eluvial/Bw horizons and an increase to around 5 in Bs horizons. This pattern is similar to the placorthods (≥ 1000 y old) in the chronosequence (Palmer *et al.* 1986). Results from our reconnaissance foliage sampling shows distinctly elevated concentrations of some nutrients for some species close to the river where the loess flux is greatest for example, for *Prumnopitys ferruginea* leaves have 1600 mg/kg P within 200 m of the river but decline to 800 mg/kg at a distance of > 600 m.

Conclusions

The highest loess flux rate (~0.05 mm/y) has a regressive effect on pedogenesis, limiting development of podsol features and maintaining a high foliar nutrient status. At 200 m downwind where loess flux rates decrease to 0.04 mm/y, this effect seems to become weaker as podsol features become more evident. A further decrease of the loess flux rate to 0.03-0.02 mm/y at 1000 m distance coincides with the first iron pans developing. Fertilisation effects as indicated by foliage nutrient status seem to reach no further than 600 m from the river. No regressive effect on soil pH was observed, suggesting rapid and strong acidification exceeding the buffer abilities of the deposited loess. Further work is currently under way to validate the rejuvenating effects of loess for additional soil and ecosystem parameters. Empirical functions relating the regressive effectiveness to loess flux rates for different soil and ecosystem parameters will be provided.

Acknowledgement

The authors acknowledge the financial support of Brian Mason Trust, Robert Bruce Trust and Lincoln University. AE is supported by a Lincoln University PhD scholarship.

References

Almond PC, Tonkin PJ (1999) Pedogenesis by upbuilding in an extreme leaching and weathering environment, and slow loess accretion, south Westland, New Zealand. *Geoderma* **92**, 1-36.

Blakemore LC, Searle BK, Daly BKN (1987) Methods for chemical analysis of soils. *Soil Bureau Scientific Report* **80**.

Burt R (Ed.) (2004) 'Soil survey laboratory methods manual.' (USDA: Lincoln).

Chadwick OA, Derry LA, Vitousek PM, Huebert BJ, Hedin LO (1999) Changing sources of nutrients during four million years of ecosystem development. *Nature* **397**, 491-497.

Chen C, Condron L, Davis M, Sherlock R (2000) Effects of afforestation on phosphorus dynamics and biological properties in a New Zealand grassland soil. *Plant and Soil* **220**, 151-163.

Dickinson KJM, Mark AF (1994) Forest-Wetland Vegetation Patterns Associated with a Holocene Dune-Slack Sequence, Haast Ecological District, South Western New Zealand. *Journal of Biogeography* **21**, 259-281.

Gibb JG (1986) A New Zealand regional Holocene eustatic sealevel curve and its application to determination of vertical tectonic movements. *Royal Society of New Zealand Bulletin* **24**, 377-395.

GNS Science (2008) Central South Island Glacial Geomorphology. (GNS Science: Wellington).

Hessel JWD (1982) The climate and weather of Westland. *N. Z. Meteorological Service Miscellaneous Publication* **115**, 1-44.

Johnson DL, Hole FD (1994) Soil formation theory: a summary of its principal impacts on geography, geomorphology, soil-geomorphology, Quaternary geology and paleopedology. In 'A Fiftieth Anniversary Retrospective Soil Science Society of America Special Publication'. (Eds R Amundson, J Harden, M Singer) pp. 111-126. (Soil Science Society of America: Denver).

Johnson DL, Watson-Stegner D (1987) Evolution model of pedogenesis. *Soil Science* **143**, 349-366.

Marx SK, McGowan HA (2005) Dust transportation and deposition in a superhumid environment, West Coast, South Island, New Zealand. *Catena* **59**, 147-171.

Palmer RWP, Doyle RB, Grealish GJ, Almond PC (1986) Soil studies in South Westland 1984/1985. Department of Scientific and Industrial Research, New Zealand, New Plymouth.

Richardson S, Peltzer D, Allen R, McGlone M, Parfitt R (2004) Rapid development of phosphorus limitation in temperate rainforest along the Franz Josef soil chronosequence. *Oecologia* **139**, 267-276.

Sowden JR (1986) Plant succession and soil development, Wanganui River catchment, South Westland, New Zealand. University of Canterbury.

Stevens PR (1968) A chronosequence of soils near the Franz Josef Glacier. University of Canterbury.

van Reeuwijk LP (Ed.) (2002) 'Procedures for soil analysis.' (ISRIC, FAO: Wageningen).

Walker TW, Syers JK (1976) The fate of phosphorus during pedogenesis. *Geoderma* **15**, 1-19.

Wardle DA, Bardgett RD, Walker LR, Peltzer DA, Lagerström A (2008) The response of plant diversity to ecosystem retrogression: evidence from contrasting long-term chronosequences. *Oikos* **117**, 93-103.

Wardle DA, Walker LR, Bardgett RD (2004) Ecosystem Properties and Forest Decline in Contrasting Long-Term Chronosequences. *Science* **305**, 509-513.

Wells A, Goff J (2006) Coastal dune ridge systems as chronological markers of palaeoseismic activity: a 650-yr record from southwest New Zealand. *The Holocene* **16**, 543-550.

Soil morphological characteristics of prairie mounds in the forested region of south-central United States

Brad Lee[A] and Brian Carter[B]

[A]Plant and Soil Sciences Department, University of Kentucky, Lexington, KY 40546, Email brad.lee@uky.edu
[B]Plant and Soil Sciences Department, Oklahoma State University, Stillwater, OK 74078, Email brian.j.carter@okstate.edu

Abstract
Prairie mounds are common in the prairie islands of the forested regions of the south-central United States, however their origin is not well understood. A topographic survey and pedon investigation of a mound and intermound area was conducted in a grassed field of prairie mounds 15 – 25 m in diameter and ~ 1 m. Both soils contain three parent materials: loess over an alluvial silty clay paleosol underlain by weathered shale. The mounded soil loess thickness is ~1.5 m while the loess in the intermound area is ~0.5 m thick. Fragic soil properties (dense, brittle, silt coats above dense horizon) are present in the loess immediately above the paleosol contact. Crayfish (*Cambarus spp*.) chimneys in the intermound and abundant gopher burrows (*Geomys spp*.) above the fragic horizon in the mound mound and loess of the intermound soil indicate the soils across the field are actively bioturbated. Depletions near the surface of the intermound soil indicate a seasonally high water table. Relict crayfish krotavinas in the paleosol under the mound and active crayfish burrows in intermound areas suggest the entire plain was previously bioturbated by crayfish. Bioturbation by gophers appears to be more recent and associated with the loess deposit.

Key Words
Prairie pimples, pimpled plains, mima mounds, Arkansas River valley

Introduction
Numerous theories exist concerning the formation of small (approximately 10 – 30 m in diameter and 0.5 – 1.5 m high) hemispherical mounds that are found in many areas of central and western North America. The unique characteristics of these mounds include an overthickened A horizon relative to adjacent soils between mounds. These mounds have been referred to as “Mima mounds”, “prairie pimples” and “pimple mounds” and the numerous theories of their genesis can be grouped into 5 categories: erosional, depositional, fossorial (burrowing animals), periglacial and seismic. It is likely that one process is hierarchically dominant in producing mounded tracts, but subordinate processes also play a role in soil development (Horwath and Johnson 2006). In the southern mid-continent Prairie mounds are common in the Arkansas River valley and the Ouachita mountains (Knechtel 1952, Seifert *et al.* 2009). The purpose of this study is to characterize soils below a mound and intermound area in the Arkansas River valley within the Ouachita physiographic province.

Methods
Environmental setting
The study site was located in 6 km east northeast of Poteau River that drains north into the Arkansas River valley. Elevation is approximately 140 m. The area has a mean annual precipitation of 1217 mm and a mean annual temperature of 16.3 C. The mound density in the field where the study site is located is approximately 9 mounds per hectare. The land use at the study site has been pasture for over 85 years.

Field
A topographic survey was conducted over a 60 x 60 m plot using a laser level to determine the determine shape and elevation of mounds relative to intermound areas. Adjacent to the plot, two pedons were described and sampled to a depth of bedrock at a mound summit and an intermound area according to standard United States Department of Agriculture – Natural Resources Conservation Service methods (Schoeneberger *et al.* 2002). Horizontal distance between the pedons is ~25 m.

Laboratory
Soil samples were dry sieved to separate coarse (20 – 75 mm), medium (5 – 20 mm) and fine (2 – 5 mm) rock fragments. Particle size distribution of the < 2 mm fraction was determined by wet sieving the sand fraction (50 µm to 2 mm) silt and clay (< 50 µm) by the pipet method (Gee and Bauder 1986). Bulk density was determined on saran-coated clods (Brasher *et al.* 1966).

1 – 6 August 2010, Brisbane, Australia. Published on DVD.

Results and discussion

Topography

The mounds are circular footprint approximately 15 to 20 m in diameter (Figure 1). The intermound area has a small 0.2 % slope toward the southwest. Other researchers have observed mid-continent prairie mounds are on gently sloping to horizontal alluvial terraces of streams and rivers (Allgood and Gray 1974; Collins 1975).

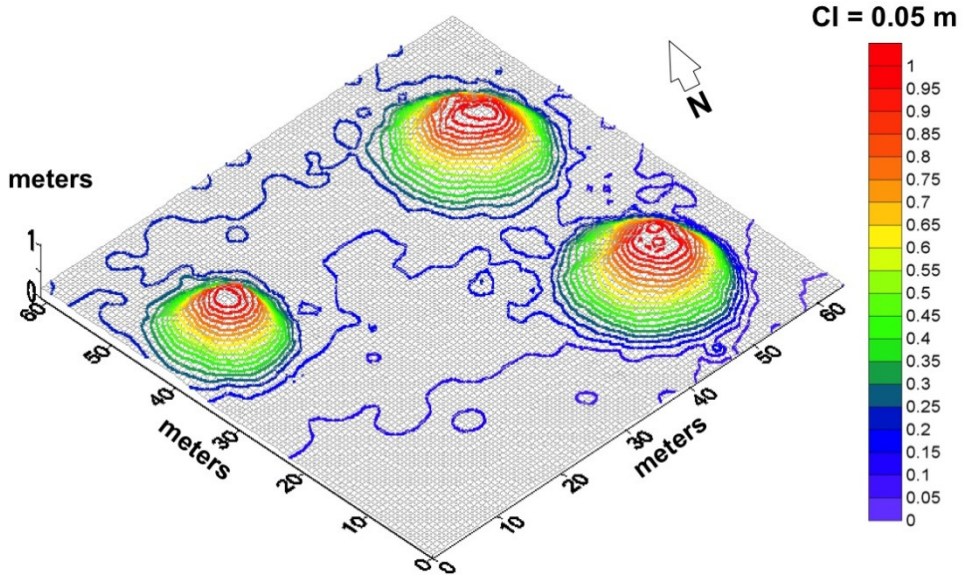

Figure 1. Topographic survey of 60 x 60 m study plot in prairie mound field.

Morphology and particle size distribution

The silt loam texture of the surface of both pedons (mound 0 – 146 cm and intermound 0 – 48 cm) suggests that the parent material of the surface is aeolian in origin (Table 1). With the exception of the brittle horizons and the dense silt loam in the mound soil (85 – 119 cm), the loess in both pedons is being actively bioturbated by gophers (*Geomys. spp.*). Between 85 – 119 cm (Bw4) of the mound soil there is a gravelly horizon (lowest D_b in subsoil = 1.22 g/cm^3 over a dense horizon (119 – 146 cm) with fragic characteristics

Table 1. Particle size distribution and texture of pedons.

		Rock fragments[A]		Sand	Coarse silt	Medium silt	Fine silt	Clay	
Horizon	Depth cm	5–75 mm	2–5 mm	50–2000 mm	20–50 µm	5– 20 µm	2–5 µm	< 2 µm	Texture
						Mound			
A1	0-26	2	13	19	35	26	7	13	Silt loam
A2	26-50	2	11	18	35	26	7	14	Silt loam
Bw1	50-70	3	8	18	36	26	7	13	Silt loam
Bw2	70-85	4	9	18	36	29	7	10	Silt loam
Bw3	85-99	2	16	18	36	28	7	11	Silt loam
Bw4	99-119	6	30	16	34	28	7	15	Fine gravelly silt loam
Bx	119-146	3	15	15	31	25	7	22	Silt loam
2Bt1	146-174	2	11	9	20	22	7	42	Silty clay
2Bt2	174-202	3	15	10	16	20	7	47	Silty clay
3Bt	202-232	4	25	9	15	19	7	50	Fine channery silty clay
3Cr	232-272	66	20	11	8	23	13	45	Extremely channery silty clay
						Intermound			
A1	0-11	1	7	10	25	32	9	24	Silt loam
A2	11-35	2	13	12	25	30	10	23	Silt loam
Bg	35-48	5	15	12	21	28	10	29	Silty clay loam
2Bt1	48-64	0	14	3	8	14	4	71	Clay
2Bt2	64-97	0	12	8	21	16	7	48	Silty clay
2Btg	97-128	4	17	9	15	20	7	49	Silty clay
3Cr	128-157	63	18	12	8	29	19	32	Extremely channery silty clay loam

[A]Rock fragments determined on weight %.

(Bx) (D_b = 1.61 g/cm^3). It appears that the Bx horizon impedes vertical water movement resulting in the formation of skeletans in the Bw4 horizon. The abrupt textural change at 146 cm coupled with paleo crayfish Krotavinas below 146 cm to a depth of bedrock suggests a period of soil development before the aeolian addition. In nearly all mid-continent occurrences, fields of prairie mounds have been noted to overlie a dense subsoil pan (claypan, fragipan) or bedrock that limits rooting at shallow depths below the intermound elevation (Knetchel 1952; Melton 1954; Horwath and Johnson 2006).

In the intermound soil, redox concentrations at the soil surface coupled with a gleyed horizon immediately above the paleosol suggest that the upper pedon is seasonally saturated during wet periods. Below 48 cm of loess, active crayfish (*Cambarus spp.*) burrows are visible. Crayfish chimneys are present on the soil surface in the intermound areas during the wet spring months. However during the late summer when these soils were sampled, there is little evidence of crayfish burrows in the loess probably due to dry season activity of gophers destroying crayfish burrows.

Table 2. Selected soil morphologic properties and bulk density of sampled horizons.

Horizon	Depth cm	Matrix color	Depletions[A]	Bulk density g/cm^3	Structure[B]	Consis-tence	Krotavinas
			Mound				
A1	0-26	10YR4/3		1.04	2 m gr	friable	20% active *Geomys*
A2	26-50	10YR4/3		1.40	2 m sbk	friable	20% active *Geomys*
Bw1	50-70	10YR5/4		1.55	1 m sbk	friable	20% active *Geomys*
Bw2	70-85	10YR5/4		1.49	1 m sbk	friable	20% active *Geomys*
Bw3	85-99	2.5Y 6/4	f,2-3,d 10YR 4/4	1.47	1 m sbk	firm, slightly brittle	10% filled *Geomys*
Bw4	99-119	10YR 5/4	m,2-3,d 10YR 8/2 skeletans	1.22	2 f sbk	very firm, brittle	
Bx	119-146	2.5Y 5/4	c,1,d, 10YR 5/6	1.61	1 f sbk	very firm	
2Bt1	146-174	10YR 4/4	c,1,p 5YR5/6	1.65	1 m sbk	very firm	10% paleo *Cambarus*
2Bt2	174-202	10YR 6/4	c,1,d 5YR 4/6 c,1,p, 2.5N	1.50	1 m sbk	very firm	10% paleo *Cambarus*
3Bt	202-232	10YR 6/4	c,1,p 7.5YR 5/8 C,1,p 2.5N	1.36	1 m sbk	very firm	10% paleo *Cambarus*
3Cr	232-272	10YR 4/3	Thin, horizontally bedded weathered shale				
			Intermound				
A1	0-11	10YR 7/3	c,1,p 10YR 5/8	1.42	2 f, m gr	friable	
A2	11-35	10YR 6/3	c,1,p 10YR 5/8	1.42	2 f sbk	friable	
Bg	35-48	10YR 7/2	c,1,p 5YR 4/4	1.38	2 f sbk	friable	20% active, filled *Geomys, Cambarus*
2Bt1	48-64	10YR 4/4	c,2,p 2.5YR 4/8	1.50	2 m sbk	firm	10% active, filled *Cambarus*
2Bt2	64-97	2.5YR 4/8	m,2,p, 10YR 6/1	1.58	2 m sbk	firm	10% active, filled *Cambarus*
2Btg	97-128	7.5YR 6/1	m,2,p 10YR 4/8	1.50	2 m sbk	firm	10% active, filled *Cambarus*
3Cr	128-157	2.5Y 4/1	Thin, horizontally bedded weathered shale				

[A] f = few, c = common, m = many, 1 = fine, 2 = medium, d = diffuse, p = prominent

[B] 1 = weak, 2 = moderate, f = fine, m = medium, gr = granular, sbk = subangular blocky

Conclusions

At this study site in the southern Arkansas River valley near the Ouachita Mountains the soils formed from a loess deposit over a silty-clay paleosol formed from alluvium over shale bedrock. About 0.5 m of loess is deposited in the intermound while 1.5 m of loess in the mounds. The mound contains a fragic horizon above the paleosol restricting water movement. Active bioturbation from gophers is prevalent in the loess above restrictive layers. Active crayfish burrowing is present in the intermound areas. The paleosol below the mound contains relict crayfish burrows suggesting that bioturbation by crayfish was a prominent soil process across this landscape in the past but is presently restricted to the intermound areas.

References

Allgood FP, Gray F (1974) An ecological interpretation of the small mounds in landscapes of eastern Oklahoma. *Journal of Environmental Quality* **3,** 37-41.

Brasher BR, Franzmeier DP, Valassis VT, Davidson SE (1966) Use of Saran resin to coat natural soil clods for bulk density and water-retention measurements. Soil Science **101**, 108.

Collins B (1975) Range vegetation and Mima mounds in north Texas. *Journal of Range Management* **28**, 209-211.

Gee GW, Bauder JW (1986) Particle-size analysis. In 'Methods of soil analysis, Part 1: Physical and mineralogical methods'. (Ed A Klute) pp. 11-34. (American Society of Agronomy: Madison WI).

Horwath JL, Johnson DL (2006) Mima-type mounds in southwest Missouri: Expressions of point-centered and locally thickened biomantles. *Geomorphology* **77**, 308-319.

Knechtel MM (1952) Pimpled plains of eastern Oklahoma. *Geological Society of America Bulletin* **63**, 689-700.

Melton FA (1954) "Natural mounds" of northeastern Texas, southern Arkansas, and northern Louisiana. *Oklahoma Geological Survey - The Hopper* **14**, 88-121.

Schoeneberger PJ, Wysocki DA, Benham EC, Broderson WD (2002) 'Field book for describing and sampling soils, Version 2.0.' (Natural Resources Conservation Service, National Soil Survey Center: Lincoln NE)

Seifert CL, Cox RT, Forman SL, Foti TL, Wasklewicz TA, McColgan AT (2009) Relict nebkhas (pimple mounds) record prolonged late Holocine drought in the forested region of south-central United States. *Quaternary Research* **71**, 329-339.

Spherites in yellow brown Kandosols in south Western Australia

Geoff Kew[A] and Bob Gilkes[A]

[A]School of Earth and Environment, University of Western Australia, Email kew.geoff@gmail.com.au, bob.gilkes@uwa.edu.au

Abstract
Spherites are strong rounded clay aggregates with characteristic internal fabrics that occur in sandplain soils in south Western Australian. Spherites are composed of dense kaolinitic clay that maybe stained with iron oxide and they are of similar size to associated quartz sand grains (mostly 250 µm to 1 mm). Four spherite types have been recognised and possible origins identified: playa spherites which are dense, smooth sided and contain clay and silt size quartz grains; regolith spherites which have a nucleus of lateritic regolith such as angular quartz grains; composite spherites which have a playa spherite nucleus which is coated with clay and iron oxide in concentric rings and with embedded quartz grains; biospherites formed by soil fauna. The abundance of each spherite type and their distribution within soil profiles has been determined and this information may assist in the interpretation of soil development on the sandplains of south Western Australia.

Key Words
Spherite, fabric, quartz grains, clay matrix, scanning electron microscopy

Introduction
Spherites (hard, round sandsize clay aggregates of various compositions) were first described for a sandplain soil from Merredin in the central wheatbelt of south Western Australia (Stace *et al.* 1968). They were considered to have formed in Tertiary laterites and had experienced minor colluvial transport. An alternative view is that spherites are wind transported lacrustrine clay derived from the surface of drying playa lakes (Killigrew and Glassford 1976). Kew and Gilkes (2010) observed spherites up 80 cm depth in a yellow brown Kandosol (Isbell 1996) from the sandplain (MacArthur 1991). Spherites were not present in the saprolitic subsoil materials indicating that spherites have an exotic origin and had been introducted into the soil profile. Observations of spherite morphology indicate that some spherites may be faecal pellets or other biologically fabricated material. To date no systematic study has been made of the morphology of spherites. This paper outlines the first description of spherite morphology for soils of the south Western Australian wheatbelt. The findings provide information on the development of sandplain soils of south Western Australia.

Methods
Sample location and sampling method
Intact cores (4 cm in diameter and 2 cm thick) were collected from yellow brown Kandosols at Bodallin in the central wheatbelt of south Western Australia. Soils were excavated to a depth of 1.5 m with a backhoe and undisturbed samples were collected from the pit face within the top 50 cm of the profile.

Polished thin sections and scanning electron microscopy
Polished thin sections of resin impregnated soil were prepared. The fabric was described using optical microscopy and the terminology of Bullock *et al.* (1985) and Kew and Gilkes (2010). Energy dispersive X-ray spectrometry (EDS) was used to determine the spatial distribution of elements in the soil clay matrix and spherites within each thin section using a Jeol 6400 scanning electron microscope operating at 15 kV with a 5 nÅ beam current. The shapes of sand grains (quartz) and spherites were measured using Image-J software (Rasband 1999) analysis of scanning electron microscope (SEM) micrographs.

Results
Occurrence of spherites
Spherites in soil profiles in south Western Australia may have originated as wind blown clay aggregates from playa lakes (Killigrew and Glassford 1976) in the paleochannel drainage system within this region (Figure 1). The current prevailing wind direction in south Western Australia is from the south west and wind blown clay would be expected to be deposited to the east of paleochannels. Bodallin is located 80 km east of a major paleochannel and spherites occur to a depth of 50 cm in these windblown sandplain soils. However, as discussed above spherites may also have been formed by other processes.
Fabric of spherites

1 – 6 August 2010, Brisbane, Australia. Published on DVD.

Thin sections of the yellow brown Kandosol at Bodallin show a class 3 fabric arrangement of clay matrix and quartz grains (Kew and Gilkes 2010). That is, greater than 50% of sand grains are coated with clay, there are 20 to 30 % structural bridges (clay) between quartz grains and there is less than 30% isolated clay matrix (Figure 2). The mean percentages of quartz grains, voids, clay matrix and spherites were measured using Image J software of scanning electron micrographs and show the soil to be composed predominately of quartz grains (39%) and clay matrix (41%) with voids (13%) and spherites (7%) being less abundant (Table 1). The sizes (feret) of quartz grains and spherites are similar (142 and 132 µm respectively) which is consistent with aeolian transport and size sorting. The mean circularity of quartz grains and spherites is the same (0.51) indicating both are somewhat elongated rather than spherical (circularity = 1). The greater variability in spherite circularity (SD = 0.13) maybe due to the varied origins of spherites.

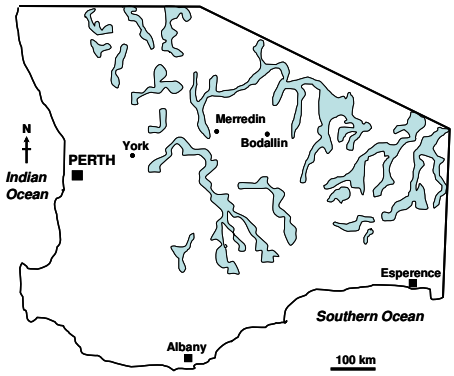

Figure 1. Paleochannels of the south Western Australian wheatbelt (McArthur 1991). Bodallin is approximately 80 km east of a major paleochannel from which spherites may have been derived.

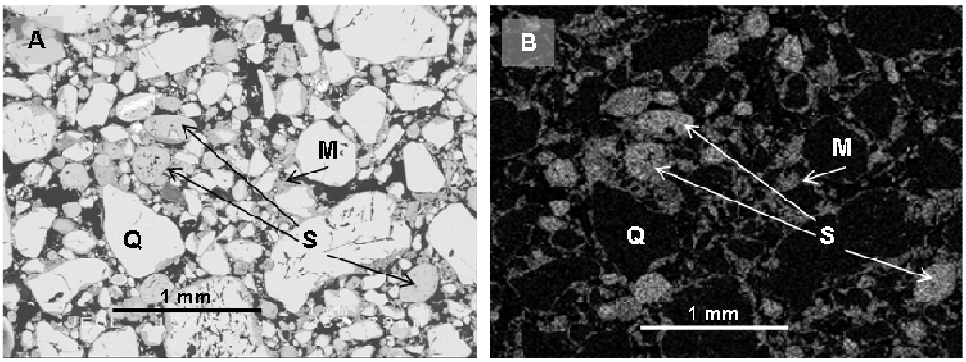

Figure 2. Representative scanning electron micrograph (A) and aluminium map (B) of a yellow brown Kandosol with class 3 fabric from Bodallin. The fabric is poorly sorted and spherites are quartz grain size. The aluminium element map shows the spherites are well rounded and their strong intensity in the aluminium map is an indication they have a higher density than the surrounding clay matrix. Q = quartz grain; S = spherite; M = porous soil clay matrix; V = void.

Table 1. Percentages of quartz grains, voids, clay matrix and spherites in 25 polished thin sections from Bodallin.

	% quartz grains	% voids	% clay matrix	% spherites
mean abundance (N=25)	39	13	41	7
SD	3	3	5	2
mean feret (µm)	142	-	-	132
SD	18	-	-	16
mean circularity	0.51	-	-	0.51
SD	0.02	-	-	0.13

EDS analysis of the clay matrix and spherites in the Bodallin soil samples shows that both materials have the ideal kaolin composition (Figure 3). That is all EDS analysis points lie on the kaolin line in the ternary plot which represents the Al_2O_3:SiO_2 ratio for ideal kaolin diluted by various amounts of Fe_2O_3. Clay matrix appears more SiO_2 rich due to embedded silt size quartz (< 20 µm) while transported spherites are Fe_2O_3 enriched. The total oxide weight percentages (Table 2) from EDS analysis are less than 100% because materials are porous (Tretyakov *et al.* 1998), so these data provide a measure of porosity in the analysed volume (Kew and Gilkes 2007). Dense clay has a higher oxide weight percent than porous clay.

Spherites are more dense (less porous) than the clay matrix of these soils which may reflect the formation of spherites in alluvial clay in playa lakes by a process of aggradation during transport over the playa surface.

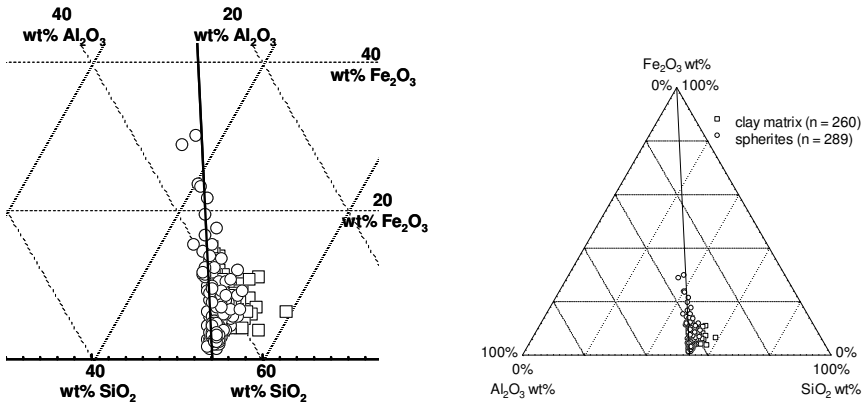

Figure 3. Normalised ternary plot of Al_2O_3, SiO_2 and Fe_2O_3 wt% determined from EDS analyses. The clay matrix and spherites of Bodallin samples are composed of kaolin clay with minor dilution by iron oxides. The kaolin line is based on the Al_2O_3:SiO_2 ratio for ideal kaolin and is represented by the line drawn to the Fe_2O_3 apex which represents kaolin mixed with increasing proportions of iron oxide.

Table 2. Mean weight percentage of Al_2O_3, SiO_2, Fe_2O_3 and oxide total (EDS spot analysis) for clay matrix and spherites from Bodallin. Spherites have a higher total oxide wt% than clay matrix which is indicative of spherites being more dense than matrix (Kew and Gilkes 2007).

	EDS weight %				Normalised oxides (∑ = 100%)			
	Al_2O_3	SiO_2	Fe_2O_3	Total Oxide	Al_2O_3	SiO_2	Fe_2O_3	N
clay matrix	27	35	5.0	68	41	52	8	260
SD	4.1	4.9	1.7	9.3	1.3	1.7	2.3	
spherite	36	43	3.5	83	43	52	5	289
SD	3.6	4.0	3.4	6.3	2.0	2.4	4.1	

Spherite morphology

A spherite classification is proposed (Figure 4). Spherites that developed in argillaceous playa lake sediments which consisted mostly of kaolinite and fine silt quartz grains have been termed "playa" spherites (micrographs A and B, Figure 4). Playa spherites are dense with little evident porosity, smooth sided and contain silt size quartz grains. These spherites are generally coated with the more porous soil matrix clay. Two types of spherites form around a nucleus of mixed origin and these are termed "regolith" spherites and "composite" spherites. Regolith spherites have fragments of granitic saprolite as a nucleus which are coated with argillaceous clay that maybe iron oxide enriched. In the example shown the clay has infilled the jagged edges of a 250 µm elongated and angular quartz grain forming a more rounded object which was subsequently transported (micrograph C). Composite spherites have a playa spherite nucleus which is commonly coated with several concentric layers of varied composition clay with embedded quartz grains (micrograph D). Spherites commonly contain more iron than the associated clay matrix, presumably because the playa clay sediment was relatively rich in iron oxide. Spherites may also have developed by biological activity within the soil and these spherites are termed "biospherites". They have distinct morphologies, for example worm cast biospherites (micrographs E and F in Figure 4) form elongated, highly porous, silt size quartz grain enriched spherites that exhibit typically extruded clay lamellae.

Conclusion

The proposed spherite classification is based on morphology and postulated origins of formation. Playa spherites are formed from argillaceous deposits, mixed spherites may have a granitic saprolite or a playa spherite nucleus which maybe coated with iron oxide rich clay and or quartz embedded clay, while biospherites have a biogenic origin. The abundance and depth of spherite types within a soil profile may help with interpreting the formation of sandplain soils.

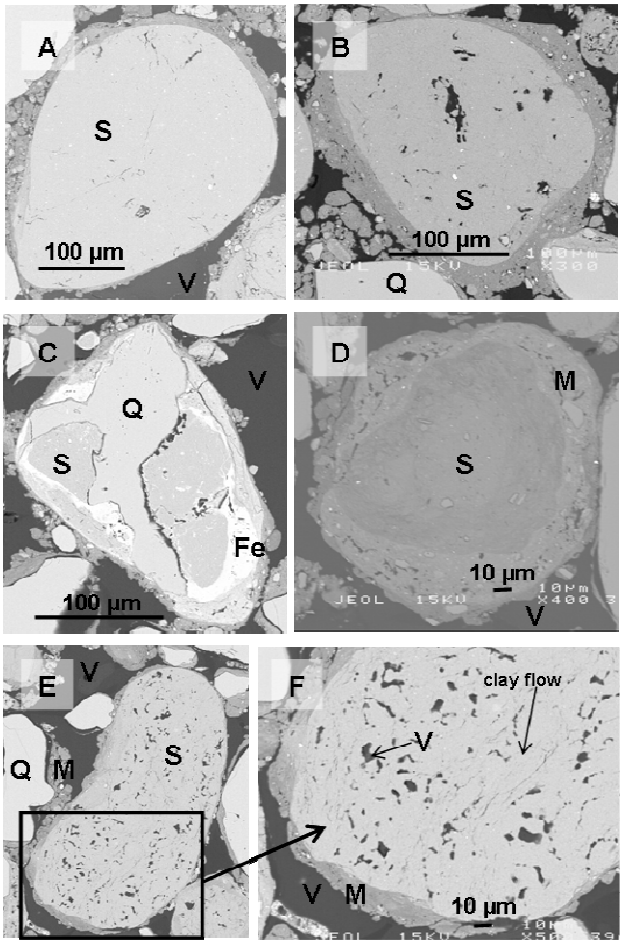

Figure 4. Spherite classification. Playa spherites are dense, smooth sided clay aggregates with minor silt size quartz grains (micrograph A and B). Mixed spherites may form with a granitic saprolite nucleus such as an angular elongated quartz grain (micrograph C) or playa spherite nucleus (micrograph D). They are commonly coated with iron rich clay or may contain consecutive rings of porous clay matrix with embedded quartz grains. Biospherites have been formed by soil fauna such as worms (micrograph E) and extruded clay flow lamellae are present (micrograph F). S = dense spherite; Q = quartz; Fe = iron enriched; M = porous soil clay matrix; V= void.

Acknowledgements

We wish to acknowledge the Grain Research Development Council (GRDC) for funding.

References

Bullock P, Fedoroff N, Jongerius A, Stoops G, Tursina T, Babel U (1985) 'Handbook for soil thin section description.' (Waine Research Publications: Wolverhampton, England).

Isbell RF (1996) 'The Australian soil classification'. (CSIRO Publishing: Melbourne, Australia).

Kew GA, Gilkes RJ (2007) Properties of regolith beneath lateritic bauxite in the Darling Range of South Western Australia. *Australian Journal of Soil Research* **45,** 1-18.

Kew GA, Gilkes RJ (2010) Relationships between fabric, water retention and strength of hard subsoils in South Western Australia. *Australian Journal of Soil Research* **48**, 167-177

Killigrew LP, Glassford DK (1976) Origin and significance of kaolin spherites in sediments of south-Western Australia. *Search* **7**, 393-394.

McArthur WM (1991) 'Reference soils of south-Western Australia'. (Australian Soil Science Society of Australia Inc. WA Branch, Perth Western Australia).

Rasband W (1999) 'Image J version 1.62.' (Research Services Branch, National Institute of Health).

Stace HCT, Hubble GD, Brewer R, Northcotte KH, Sleeman JR, Mulcahy MJ, Hallsworth EG (1968) 'A handbook of Australian Soils' (Rellim Technical Publication 206. Rellim Technical Publications, Glenside).

Tretyakov VV, Romanov SG, Fokin AV, Alperovitch VI (1998) EMPA of the composition of opal-based nanostructured materials. *Mikrochimica Acta, Suppl* **15**, 211-217.

Sydney gets a dusting, but what's in it?

Stephen Cattle

Faculty of Agriculture, Food and Natural Resources, The University of Sydney, NSW, Australia, Email s.cattle@usyd.edu.au

Abstract
During late September 2009, a series of spectacular dust storms moving across eastern Australia and out into the Tasman Sea. One of these dust storm events (September 23rd, 2009) was so severe that it reduced visibility in the city of Sydney to several hundred metres. Such an event offers a rare insight into the conditions that must have prevailed during the arid, glacial periods of the late Pleistocene, when significant aeolian dust deposits are thought to have formed across southern New South Wales (NSW). Deposited dust in Sydney and two inland NSW locations was analysed for particle size characteristics, morphological features and mineral suite. The dust deposited in Sydney, estimated as being around 4 t/km^2 for the event, was very fine, yet contained relatively little clay; the mineral suite was dominated by quartz, with small amounts of iron oxides, kaolinite and illite. For the deposited dust collected in inland NSW, the modal particle sizes were somewhat coarser than those of the Sydney dusts, but other attributes were similar. The transport mode for the dust deposited in Sydney appears to have been primarily particulate, unlike the assumed aggregated mode of transport for the ancient dusts deposited in southern NSW.

Key Words
Aeolian dust, parna, loess, particle size, transport distance

Introduction

In Australia, loess deposits have rarely been reported. Instead, most of the literature reporting aeolian deposits has discussed "parna", a red, clayey material believed to have been formed in deposits laid down during arid phases of the late Pleistocene. The source of this material is presumed to have been the semi-arid lands of northwestern Victoria and the arid lands of western NSW and eastern South Australia. A further assumption regarding this material is that it was transported as silt-sized aggregates of clay and calcium carbonate, along with some companion grains of quartz (Butler, 1956). As noted by Hesse and McTainsh (2003), however, there is scant evidence of either the age(s) or transport mode(s) of this material. During 2009, the western districts of NSW and the Lake Eyre Basin of South Australia experienced a period of prolonged dryness. In the month of September, a series of fast-moving frontal systems swept from west to east across Australia, pushing erosive winds over desiccated landscapes. On Tuesday, September 22nd and Wednesday, September 23rd, large dust plumes engulfed Canberra and Sydney, respectively. In Sydney, the dust plume arrived in the pre-dawn hours of September 23rd and had reduced visibility to several hundred metres by about 7 am. At 9 am the visibility in the city of Sydney was approximately 2 km, and by 2 pm the dust had largely cleared. As this remarkable dust storm provided a rare insight into conditions that presumably prevailed during the previous arid, glacial periods, a number of deposited dust samples were collected in Sydney during and after the event for analysis. Of particular interest was the apparent mode of transport of the dust – did it travel largely as particulates or as aggregated entities? Also, what sizes were the dust grains/aggregates, what were the main minerals in these dusts, and how do these dusts compare to the pedogenically altered dusts that comprise "parna"?

Methods

Deposited dust samples collected

A number of deposited dust samples were opportunistically sampled from car windscreens and verandah surfaces in Sydney during, or shortly after, the dust storm of Wednesday, September 23rd. Similarly, deposited dust samples were taken from previously clean, exterior surfaces of buildings near the central western NSW town of Orange and the southern NSW town of Albury, shortly after the dust storm event of September 23rd. On the morning of the dust storm, three open-topped trays containing glass beads were positioned on the rooves of multi-storey buildings on the campus of The University of Sydney to act as dust traps. These dust traps were removed the following morning and the trapped dust washed off the marbles before being slowly oven-dried.

Measurement and analyses of the deposited dust
For the opportunistically sampled dust deposits, small sub-samples were assessed for particle-size distribution using a Coulter Multisizer 3. The micromorphological features of these dusts were determined and recorded using a scanning electron microscope, while for those dust samples of sufficient mass, the mineral suite was determined qualitatively using X-ray diffraction analysis. A conservative estimate of dust deposition rate in Sydney was made by doubling the amount captured by the traps, as the period of poorest visibility occurred in the 3 hours prior to installation of the traps.

Results
The dust that fell onto Sydney on the morning of Wednesday, September 23rd, 2009 was remarkably fine. As indicated in the particle size distributions in Figure 1, the dust particles falling onto car windscreens up to 9 am, and between 9 am and 12 pm that day, have modal diameters of around 18 µm and 5 µm. Interestingly, the finer population appeared to increase in proportion as the morning wore on (cf. Figures 1a and 1b), despite the fact that windspeeds picked up during the morning and visibility gradually improved. Although the Coulter Multisizer does not effectively measure clay-sized particles, the notable presence of particles 2-5 µm in diameter, particularly in the windscreen dust deposited between 9 am and midday, suggests the concomitant presence of clay-sized material. This was confirmed when dust samples were viewed under the scanning electron microscope, with clay-sized particles found to be adhering to fine silt-sized grains of quartz. Particulate dust appeared to be more common than strongly aggregated dust.

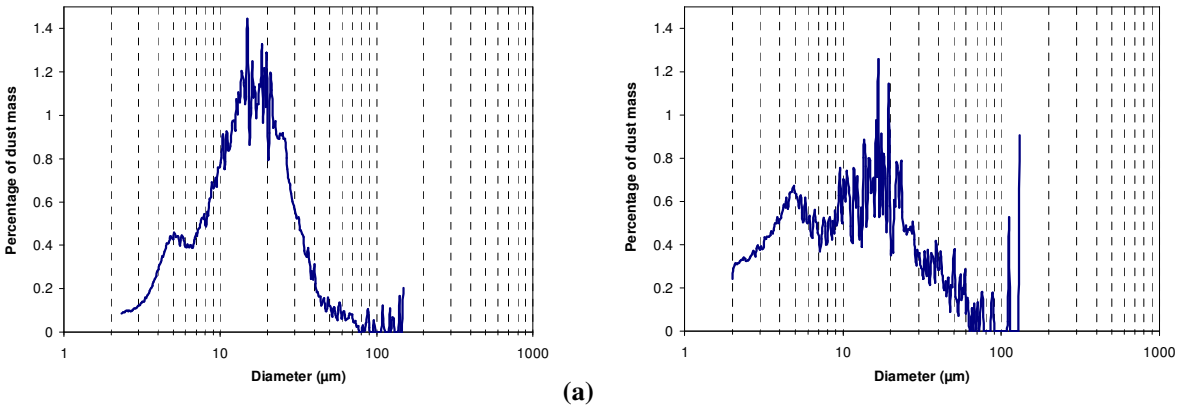

Figure 1. High-resolution particle size distributions of deposited dust samples obtained from a car windscreen at The University of Sydney at (a) 9 am and (b) 12 noon, on Wednesday, September 23rd, 2009.

The dusts sampled at Orange and Albury was distinctly coarser than the Sydney dust (modes between 20 and 30 µm), but there were still minor populations of finer (5-20 µm) particles. This difference in dominant particle size is reflection of the distance travelled from source. Mineralogically, the dusts collected in Sydney, Orange and Albury are relatively uniform, consisting primarily of quartz, with smaller contributions of iron oxides, kaolinite and illite. Calcium carbonate, a prominent component of the "parna" conceptual model, was not present in any of the dust samples. The contribution of iron oxides to the dust that engulfed Sydney is likely to have been temporally variable. In the first few hours after sunrise, the suspended dust was distinctly reddish-brown in colour, whereas by mid-morning the suspended dust was light brown in colour. Verification of this dust colour change is provided by comparison of the deposited dust samples collected after 9 am with those samples including dust from the entire event; the whole event dust samples are red-brown, whereas the post-9 am samples are light brown. Presumably this colour difference is a result of different source areas contributing sediment to the different parts of the air cell moving across NSW the preceding night.

Only a conservative estimate can be made of the dust deposition amount in Sydney on September 23rd because dust traps were not installed on building rooves until 9 am, by which time the suspended dust had thinned somewhat. Nevertheless, the three traps installed captured between 1 and 2 g dust/m^2, which equates to between 1 and 2 t dust/km^2. As the windspeed increased during the morning, it could reasonably be expected that deposition was greater before 9 am than after, so doubling the post-9 am amount (to 4 t dust/km^2) would seem to be a plausible, conservative estimate of total dust deposition. Whilst this is not a large deposit by global standards, it represents about a half of the annual dust deposition measured at a number of other Australian sites (Cattle *et al.* 2009).

Conclusion

The spectacular dust storm that engulfed Sydney on September 23rd 2009 offered a glimpse of the conditions that must have prevailed during the arid glacials of the late Pleistocene. It is thought that aeolian dust deposits of southern NSW were laid down during these arid glacial periods, but there has been conjecture over the form of the transported dust and the degree of pedogenesis of this sediment. Dust samples collected from around Sydney and from two inland NSW locations were generally very fine-grained, but not particularly well aggregated. Mineralogically, these dust samples are dominated by quartz, with small amounts of iron oxide, kaolinite and illite. Calcium carbonate does not feature prominently in any of the dust samples. Overall, the dust transported in this event does not strongly conform to the conceptual model of "parna" which took hold in Australia in the 1950s.

References

Butler BE (1956) Parna - an aeolian clay. *Australian Journal of Science* **18**, 145–151.

Cattle SR, McTainsh GH, Elias S (2009) Æolian dust deposition rates, particle-sizes and contributions to soils along a transect in semi-arid New South Wales, Australia. *Sedimentology* **56**, 765–783.

Hesse PP, McTainsh GH (2003) Australian dust deposits: modern processes and the Quaternary record. *Quaternary Science Reviews* **22**, 2007–2035.

What is the effect of loess on soil catena evolution in the Midwestern United States?

Peter M. Jacobs[A], Joseph A. Mason[B], and Paul R. Hanson[C]

[A]Department of Geography and Geology, University of Wisconsin-Whitewater, Whitewater, WI, USA, Email jacobsp@uww.edu
[B]Department of Geography, University of Wisconsin-Madison, Madison, WI, USA, Email mason@geography.wisc.edu
[C]School of Natural Resources, University of Nebraska-Lincoln, Lincoln, NE USA, Email phanson2@unl.edu

Abstract
We investigate the influence of loess on soil catena development, specifically, soil morphological expression and biogeochemical processes associated with profile development. Loess has a positive impact on solum thickness and development of clay-enriched subsoil horizons. Abundant pore space and reactive surface area associated with the high silt and clay content and smectitic clay mineralogy of the loess in our study areas aids moisture retention, biogeochemical transformations and translocation of Fe and P, and storage of C, especially with increasing carbonate mineral content.

Key Words
Colluvium, Alfisols, Mollisols

Introduction
In the Midwestern United States loess accumulated on land surfaces not covered by glaciers and also on some glaciated land surfaces following exposure from beneath the ice. In most areas, the loess was redistributed down slopes, leading to a patchwork in which parts of the landscape have thick loess, thin loess, or no loess at all. The hypothesis tested in this project is that the thickness of loess remaining in a given location has a major influence on soil development because of the distinctive properties of the loess, which should favor high moisture and nutrient retention and rapid formation of clay-rich subsoil horizons.

In this paper we investigate the influence of loess on soil catena evolution in two distinct landscape types in the Midwest. Our study areas include (1) the steeply sloping bluff lands of the Upper Mississippi Valley in southeastern Minnesota, where slopes consist of Pleistocene periglacial slope deposits (colluvium) that vary in the proportion of mixed loess and carbonate bedrock or sandstone bedrock, and (2) the glaciated land surface of the Green Bay Lobe in south-central Wisconsin that has landscape characterics varying from steeply sloping drumlinized terrain to low relief till and outwash plains.

Methods
Soil catenas on the Green Bay Lobe land surface were sampled using a Giddings hydraulic soil corer, extracting 7.6 cm cores. Colluvial soil catenas in the bluff lands were sampled from outcrops created by recent excavations for logging roads. Soils were described using standard terminology and sampled by genetic horizon for laboratory analysis. Lab analyses followed standard methods and included: particle size analysis by pipet and sieve and laser diffraction, soil organic carbon (SOC) by loss-on-ignition, pH using 1:1 soil-water paste, Fe oxyhydroxides by dithionite and oxalate extractions and analyzed by atomic absorption, P fractions by sequential extractions, base cations, acidity and ECEC by ammonium acetate and KCl extractions, and clay (<2 μm) and silt (8-63 μm) mineralogy by x-ray diffraction.

Results
Minnesota Bluff Lands
The soils at our Cut Across Road research site occur on a steep slope underlain by bedrock at a fairly shallow depth, including dolomite of the Prairie du Chien Group (Ordovician) underlying the upper part of the slope, and sandstone of the Jordan Formation (Cambrian) beneath the lower slope. All of the soils that were sampled formed from various mixtures of loess and weathered bedrock. The loess is dominated by silt, but contains significant amounts of smectite clays (Mason *et al*. 1994). Both of these materials have been moved some distance downslope by erosion and deposition, primarily during the last glacial period, from about 25,000 to 11,500 years ago.

1 – 6 August 2010, Brisbane, Australia. Published on DVD.

The soils can be divided into three groups. Silt-rich Group 1 soils on the very gently sloping, lowest part of the slope are formed mainly from redistributed loess, with some sand input from weathered sandstone. These silty soils have not yet been studied in detail. Higher on the concave lower slope, Group 2 soils are formed predominantly in sand weathered from sandstone, though with a silty loess-derived layer in one profile. These sandy soils have acidic upper horizons and low contents of organic carbon that is concentrated in a thin A horizon, and relatively low water retention and potential to supply nutrients. Group 3 soils occur on the steep, convex upper slope, and have upper horizons formed in a mixture of loess and dolomite rock fragments. Near the ridgetop, subsoil horizons are formed in the same material, but farther downhill, subsoils are formed from weathered sandstone. All of these upper slope soils have neutral to alkaline pH and have silt- and smectitic clay-rich near-surface horizons that have relatively high potential to store SOC (Figure 1). Many of the upper slope soils contain abundant organic carbon and phosphorus (mainly in organic matter). While all of these properties may suggest that the upper slope soils are favorable for high plant productivity, availability of some nutrients may actually be seriously limited by high pH, slow organic matter decomposition, and low total volume of water storage because of abundant rock fragments.

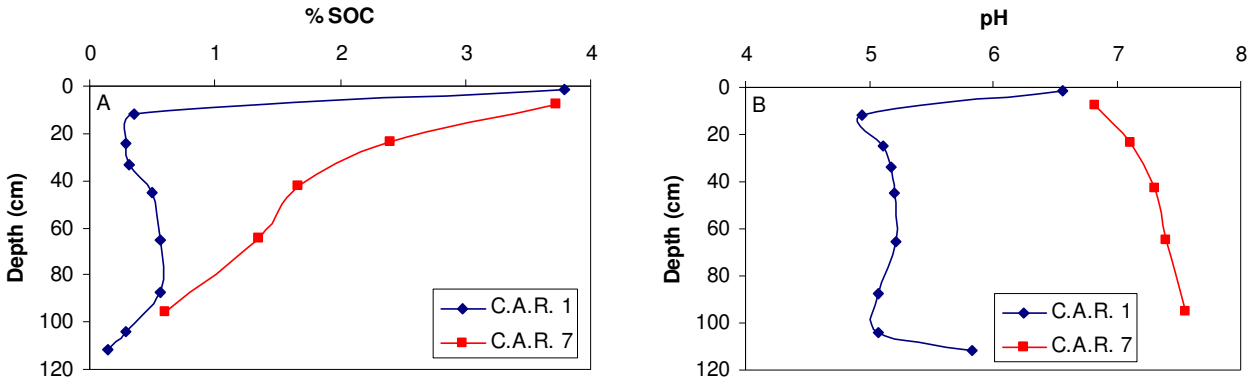

Figure 1. Profile distribution of SOC and pH in soils in Groups 2 and 3. Group 2 soils (C.A.R. 1) have low silt and carbonate bedrock content and are acid, and store less SOC than Group 3 soils (C.A.R. 7) with higher silt and carbonate bedrock components.

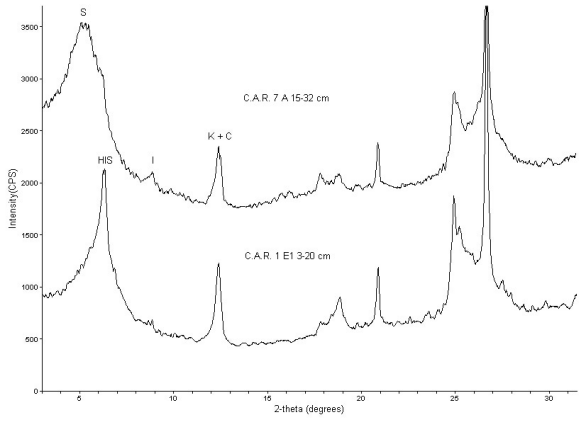

Figure 2. X-ray diffractograms of <2 µm clay minerals from soil profiles formed in sandy colluvium with minimal loess (C.A.R. 1) and mixed loess and dolomitic colluvium (C.A.R. 7). Note the strong 1.4 nm peak associated with the acidified sandy colluvium, while the minimally acidified C.A.R 7 sample retains the distinctive smectite peak characteristic of loess. Heat treatments (not shown) confirm the presence of HIS/HIV. Samples were Mg saturated and ethylene glycol solvated; S=smectite, HIS=hydroxy interlayered smectite, I=illite, and K+C=kaolinite plus chlorite.

C.A.R. 1 is acidic throughout the profile (Figure 1), especially below the thin A horizon, making clay, iron, and phosphorus mobile within the soil. Clay coatings and iron oxides have been translocated from a relatively thick (38 cm) eluvial upper solum to the Bt horizon. In contrast, the degree of acidification in C.A.R. 7 is minimal, and dolomite is still present in the silt fraction. Profile morphology consists of a series of dark horizons (A/AB/Bw) with minimal evidence of clay translocation. Clay mineral weathering is not detectable in C.A.R. 7, while in the acid profile C.A.R 1, smectite has developed hydroxy interlayers (Figure 2).

Green Bay Lobe

Soils on the Green Bay Lobe land surface have formed in a range of loess thickness from zero to nearly two meters overlying glacial sediment. Loess accumulated following deglaciation of the region. Regional thickness and grain-size fining patterns indicate the source of the loess was largely the drained bed of Glacial Lake Wisconsin, along with clays from sources further west, based on the content of smectite clay minerals. Much of the loess accumulated between 14,000-10,600 cal yrs BP, based on optical stimulated luminescence ages of eolian sand in the source area (Rawling *et al.* 2008), although this project reports some sand dunes on the Green Bay Lobe land surface were active until at least 9500 cal yrs BP.

Following deposition, loess was commonly redistributed in the landscape, with steeper slopes retaining minimal to no loess. Most of the redistributed loess accumulated in foot slope positions, filling topographic lows between drumlins. In addition, drainage of the underlying landscape apparently affected loess redistribution, with permeable outwash deposits or fractured bedrock uplands retaining uniformly greater thickness of loess. Thickness patterns of loess strongly impact the uniformity of mapped soil patterns and profile characteristics such as solum thickness and Bt horizon expression.

For example, flat outwash plains abandoned as terraces accumulated loess with minimal redistribution and soil surveys show large soil bodies with similar profile characteristics. A catena transect across a former braid channel demonstrated minimal variation in loess thickness and only slight changes in soil morphology associated with increased wetness in the braid channel. In drumlinized terrain, the loess was redistributed into the intervening lowlands, and soils are formed in loess and till on summit and backslope positions, while in footslope positions the entire solum is contained within loess (Figure 3).

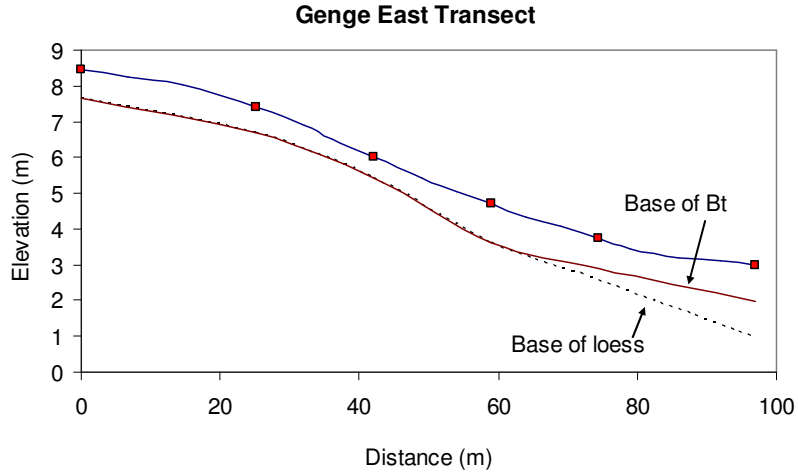

Figure 3. Cross section along a drumlin hillslope illustrating surface elevation, location of profile descriptions (■) field-identified thickness of loess mantle, and base of Bt horizon. Note coincidence of loess mantle and Bt horizon expression, while in footslope position loess thickness exceeds Bt thickness.

The influence of the loess mantle on profile expression is illustrated in Figure 4, where thickness of the loess mantle has a clear impact on the thickness of the solum and to a lesser extent the thickness of Bt horizons. Clay enriched subsoil (Bt) horizons occur in nearly all soils on the Green Bay Lobe land surface. The presence of illuvial upper sola is largely a function of native vegetation, with only forest areas typically having relatively thick E horizons. Clay minerals in the loess are dominated by smectite (Figure 5).

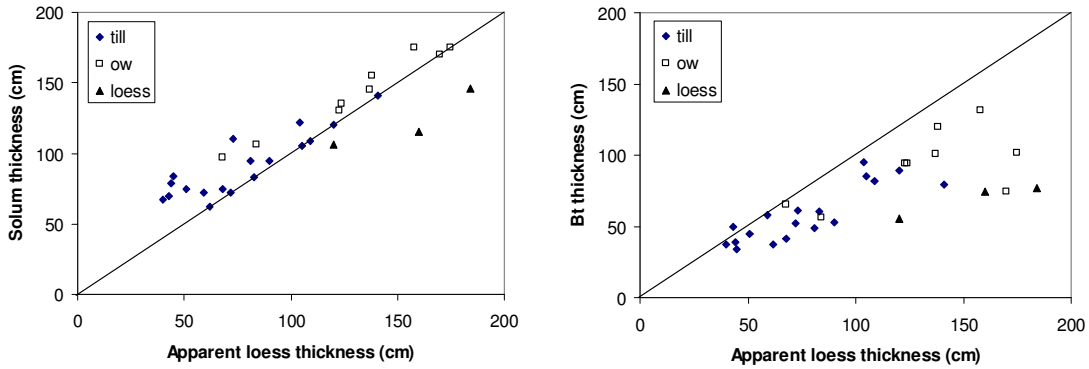

Figure 4. (Left) solum thickness as a function of loess thickness follows a near 1:1 relationship in soil formed in a mantle of loess over till, outwash, or entirely in loess. Note in most instances solum thickness exceeds thickness of the loess mantle because soil formation has transgressed the lithologic discontinuity. (Right) Thickness of Bt horizons increase as loess thickness increases, although at a lesser rate than solum thickness.

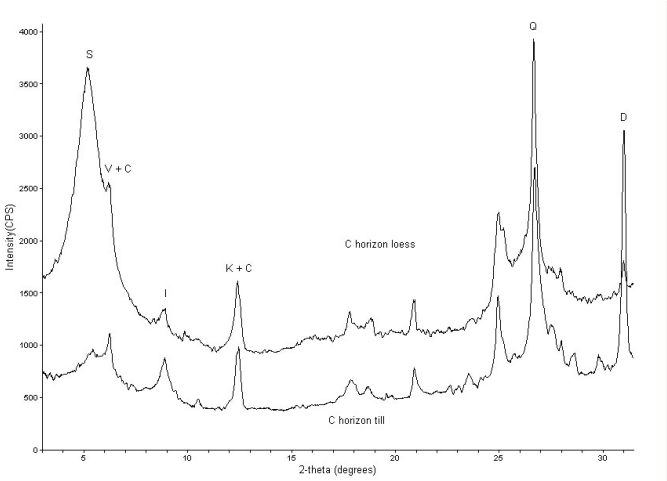

Figure 5. X-ray diffractograms of <2 µm clay minerals from C horizons in loess (upper) and till (lower) on the Green Bay Lobe land surface. Note the distinctive peak associated with smectite in loess, while till has greater amounts of illite and kaolinite, along with very abundant dolomite (in all size fractions). Samples were Mg saturated and ethylene glycol solvated; S=smectite, V+C=vermiculite plus chlorite, I=illite, K+C=kaolinite plus chlorite, Q=quartz, and D=dolomite.

Discussion

Loess is a widespread soil parent material of soils of the mid-continent of North America and elsewhere. Redistribution of loess under periglacial climate conditions established the parent materials for soil formation and much of the geographic variability of solum thickness and morphology in catenas of the upper Midwest U.S. The abundance of silt and smectite clay in loess deposits provides abundant pore space and reactive surfaces for soil formation and ecosystem processes. Increasing content or thickness of loess in soils, especially in the presence of carbonate minerals greatly enhances soil storage of water, SOC, nutrients, and buffering against acidification.

References

Mason JA, Nater EA, Hobbs HC (1994) Transport direction of Wisconsinan loess in southeastern Minnesota. *Quaternary Research* **41**, 44-51.

Rawling JE, III, Hanson PR, Young AR, Attig JW (2008) Late Pleistocene dune construction in the Central Sand Plain of Wisconsin, USA. *Geomorphology* **100**, 494-505.